UNIVERSIDADE DE SÃO PAULO
INSTITUTO DE QUÍMICA
Programa de Pós-Graduação em Ciências Biológicas (Bioquímica)

TÚLIO FELIPE PEREIRA

Papel da proteína Ectodermal-neural cortex 1 (ENC1) na progressão de glioma humano, identificação de um peptídeo internalizado por células de glioblastoma humano e desenvolvimento de um método alternativo para gerar curvas de crescimento celular.

Versão corrigida da Tese defendida.

São Paulo

Data do Depósito na SPG:
10/10/2018

TÚLIO FELIPE PEREIRA

Papel da proteína Ectodermal-neural cortex 1 (ENC1) na progressão de glioma humano, identificação de um peptídeo internalizado por células de glioblastoma humano e desenvolvimento de um método alternativo para gerar curva de crescimento de células.

Tese apresentada ao Instituto de Química da Universidade de São Paulo para obtenção do Título de Doutor em Ciências Biológicas (Bioquímica)

Orientadora: Profa. Dra. Mari Cleide Sogayar
Co-orientadora: Profa. Suely K N Marie

São Paulo
2018

Autorizo a reprodução e divulgação total ou parcial deste trabalho, por qualquer meio convencional ou eletronico, para fins de estudo e pesquisa, desde que citada a fonte.

Ficha Catalográfica elaborada eletronicamente pelo autor, utilizando o programa desenvolvido pela Seção Técnica de Informática do ICMC/USP e adaptado para a Divisão de Biblioteca e Documentação do Conjunto das Químicas da USP

Bibliotecária responsável pela orientação de catalogação da publicação:
Marlene Aparecida Vieira - CRB - 8/5562

P436p

Pereira, Túlio Pereira
Papel da proteína Ectodermal-neural cortex 1 (ENC1) na progressão de glioma humano, identificação de um peptídeo internalizado por células de glioblastoma humano e desenvolvimento de um método alternativo para gerar curvas de crescimento celular / Túlio Pereira Pereira. - São Paulo, 2018.
85 p.

Tese (doutorado) - Instituto de Química da Universidade de São Paulo. Departamento de Bioquímica.
Orientador: Sogayar, Mari Cleide
Coorientador: Marie, Suely K N

1. Ectodermal-neural cortex protein 1. 2. prognóstico clínico. 3. peptídeo LHTNELQ. 4. peptídeos internalizados por glioblastoma humano. 5. curva de crescimento celular. I. T. II. Sogayar, Mari Cleide, orientador. III. Marie, Suely K N, coorientador.

Dedicatória

À minha amada “Vó Dita”, que faleceu vítima de um glioma.

À minha amada “Tia Maria”, que faleceu vítima de um câncer de mama metastático.

À minha amadíssima prima Rita de Cássia e à amiga Débora Cristina, que também já não estão mais por perto.

A vocês dedico este trabalho.

AGRADECIMENTOS

Agradeço, primeiramente, às agências de fomento: Conselho Nacional de Desenvolvimento Científico e Tecnológico (CNPq) e a Fundação de Amparo a Pesquisa do Estado de São Paulo (FAPESP Processo N° 2016/01626-9), que me sustentaram financeiramente ao longo deste doutorado.

À minha amada mãe, que sempre me trilhou no caminho da educação e da busca pelo crescimento, pouco adianta eu tentar expressar o tamanho da minha gratidão. Minha base, meu amor pelo conhecimento e pela descoberta, tudo isso vem de uma sementinha por ela plantada desde minha educação primaria, pelo método construtivista, que ela tanto admira.

Ao meu amado pai, por na sua discrição ter me amado sempre. Obrigado por ter acreditado e torcido muito por mim.

Ao meu amor, Arielle, minha amadíssima esposa, que me apoiou em todos os meus projetos. Magnífica esposa, parceira, mãe e mulher, sempre ao meu lado. Tantas vezes morreu pra si, pra fazer-me vivo nos meus sonhos. Que eu possa retribuir-la por isso.

Aos meus irmãos Bruno, Leidy & Adriano e Ilsa & Marcos, que sempre me impulsionaram. Muito obrigado Leidy & Adriano por ter me ajudado a me manter em São Paulo no início do Doutorado.

Ao meu amadíssimo filho Samuel, que me estimulou simplesmente por existir, e me encantou e encanta a cada sorriso. Obrigado por me mostrar todos os dias como amar é essencial para a realização do homem.

É preciso aqui fazer uma nova menção à minha mãe, e me ajudou muito a mantermo-nos em São Paulo após o nascimento do Samuel.

A minha aluna de Iniciação Cientifica Amanda Caodaglio e aos Doutores Marcos Demasi, Lauren Camargo e Renato Astorino, que foram fundamentais para a realização deste trabalho.

A minha orientadora Dra Mari Sogayar, que me proporcionou a oportunidade de me aventurar pelo fantástico mundo da ciência.

A minha co-orientadora Dra. Suely Marie, pela concessão das amostras que foram fundamentais para o desenvolvimento deste projeto.

A Dra Renata Pasqualini e Dr Wadih Arap e demais membros do A/P Lab, que me proporcionaram e me auxiliaram durante meu estágio na Universidade do Novo México - EUA. Agradeço novamente aqui a Dra Mari Sogayar, que foi fundamental na viabilizaçao deste estágio.

A Deus, por ter criado o mundo de maneira tão intrigante e perfeita, e por dar aos cientistas a oportunidade de contemplar minusciosos detalhes, que tantas pessoas nascem e morrem sem conhecer.

Ao Instituto de Química da USP, por sua excelência na formação de doutores.

Aos marmotas, tchurubiros, e tantos outros Nucelianos que me acompanharam no dia a dia do trabalho cientifico, dividindo frustrações e alegrias, desesperos e “eurekas”.

Aos técnicos do Laboratorio, Zizi, Débora, Alan, Mônica e Amanda, que muito me auxiliaram.

Meus amigos, uma falsa ciência gera ateus, mas a verdadeira ciência leva os homens a se curvar diante da divindade...

Voltaire

RESUMO

Pereira, T. F. **Papel da proteína Ectodermal-neural cortex 1 (ENC1) na progressão de glioma humano, identificação de um peptídeo internalizado por células de glioblastoma humano e desenvolvimento de um método alternativo para gerar curvas de crescimento celular.** 2018. 86p. Tese - Programa de Pós-Graduação em Bioquímica. Instituto de Química, Universidade de São Paulo, São Paulo.

Gliomas são a forma mais comum de malignidades primárias intracranianas, dentre os quais os astrocitomas são os mais frequentes. A proteína Ectodermal-neural cortex 1 (ENC1), também conhecida como Nuclear Restricted Protein/Brain (NRP/B), foi primeiramente caracterizada como uma proteína que interage com o citoesqueleto por meio de ligação à actina através de domínios Kelch-like, sendo relacionada com diferenciação neuronal durante o desenvolvimento do sistema nervoso. O primeiro capítulo desta tese descreve confirmação da capacidade supressora tumoral de ENC1 por abordagem de edição genômica, analisa a expressão de ENC1 em um conjunto de amostras de pacientes com gliomas e correlaciona esses dados com tempo de sobrevida geral e sobrevida livre de progressão tumoral nos pacientes, concluindo que a expressão de ENC1 pode ser utilizada como um biomarcador da agressividade do glioma. O segundo capítulo apresenta a identificação e caracterização *in vitro* do peptídeo LHTNELQ, que foi selecionado pela metodologia de *Phage display* utilizando-se de células de glioblastoma humano. Este novo peptídeo é capaz de internalizar-se nestas células e figura como uma nova ferramenta para o desenvolvimento de estratégias terapêuticas para glioblastomas. No terceiro capítulo propõe-se um método alternativo para gerar curvas de crescimento celular de cultura aderente, o qual é baseado no decaimento da fluorescência do reagente CFSE ao longo do tempo. Trata-

se de um método alternativo para a determinação de curvas de crescimento de culturas aderentes, com menor variação entre as réplicas técnicas do que os métodos baseados em contagem das células.

Palavras-chave: Proteína ectodermal-neural cortex 1 (ENC1); prognóstico clínico; peptídeo LHTNELQ; peptídeo endereçado a glioblastoma humano; método independente de contagem baseado em fluorescência; curvas de crescimento celular.

ABSTRACT

Pereira, T. F. **Role of Ectodermal-neural cortex 1 protein in human glioma progression, identification of a peptide internalized by human glioblastoma cells and development of an alternative method to generate growth curves of adherent cultures**. 2018. 86p. PhD Thesis – Graduate Program in Biochemistry. Instituto de Química, Universidade de São Paulo, São Paulo.

Gliomas are the most common form of primary intracranial malignancy, among which astrocytomas are the most frequent. Ectodermal-cortex protein 1 (ENC 1), also known as Nuclear Restricted Protein/Brain (NRP/B), was first characterized as a protein which interacts with the cytoskeleton by binding to actin through Kelch-like domains, being related to neural fate specification during development of the nervous system. The first chapter of this thesis confirms ENC1 as a tumor suppression properties by a genomic edition approach, analyses ENC1 expression in a set of patient glioma samples and describes the correlation these data with patients survival and progression-free survival, concluding that ENC1 expression may constitute a biomarker for glioma aggressiveness. The second chapter refers to the identification and *in vitro* characterization of the LHTNELQ peptide, which was selected by the Phage Display method using human glioblastoma cells. This new peptide is able to be internalized by these cells and features as a new tool for the development of glioma therapeutics. The third chapter report an alternative method to generate growth curves of adherent cell cultures, which is based on the CFSE fluorescence decay over time. It is an alternative method to determine growth curves of cultured cells, with smaller variation among technical replicates than that of counting-based methods.

Keywords: Ectodermal-neural cortex 1 protein (ENC1); patient prognosis; LHTNELQ peptide; human glioblastoma targeted peptide; Counting-free fluorescence based method; cell growth curve.

SUMMARY

1. General Introduction 14

2. Upregulation of tumor suppressor Ectodermal-neural cortex 1 protein (ENC1) during human glioma progression is associated with unfavorable patient prognosis. 20

2.1. Introduction 20

2.2. Materials and Methods 22

2.2.1. Cell culture 22

2.2.2. Generation of ENC1-edited U87MG cell line 22

2.2.3. T7 endonuclease assay 22

2.2.4. Characterization of ENC1 random editions by Sanger sequencing 23

2.2.5. Clonogenic potential assay 23

2.2.6. Cell cycle assay 24

2.2.7. Cell growth curves 24

2.2.8. In vivo tumorigenic potential 24

2.2.9. Analysis of ENC1 expression in patient glioma samples 25

2.2.10. Public data in silico analysis 26

2.3. Results 27

2.4. Discussion 34

2.5. Conclusions 37

3. Identification and *in vitro* characterization of a novel peptide internalized by human glioblastoma cells. 38

3.1. Introduction 38

4. Materials and Methods 40

4.1.1. Cell culture 40

4.1.2. Biopanning 40

4.1.3. Internalization assay 40

4.1.4. Phage binding assay 41

4.1.5. Immunofluorescence microscopy 41

4.1.6. Alanine scanning 42

4.1.7. Competition assay 42
4.1.8. Statistical analysis 42
4.2. Results 43
4.3. Discussion 50
4.4. Conclusions 52
5. Counting-free fluorescence-based method to generate growth curves of adherent cell cultures. 53
5.1. Introduction 53
5.2. Materials and Methods 56
5.2.1. Cell culture 56
5.2.2. Cells staining with CFSE 56
5.2.3. Growth curves 56
5.2.4. Manual cell counting using the Neubauer Chamber. 57
5.2.5. Automatic cell counting using the Z2 Coulter Counter Analyzer (Beckman Coulter) 57
5.2.6. Automatic cell counting using the Accuri C6 Cytometer (BD Biosciences) . 57
5.2.7. CFSE signal measurement using the Accuri C6 Cytometer (BD Biosciences) 58
5.2.8. Doubling time calculation 58
5.2.9. Statistical Analysis 58
5.3. Results 60
5.4. Discussion 68
5.5. Conclusion 70
6. Final conclusions 73

1. General Introduction

The Central Nervous System (CNS) is the main responsible for integration of vital functions in vertebrates, being sensitive to several biochemical stimuli from other organs and accordingly reacting to stimuli, by orquestrating and integrating the entire biological system. The CNS is constituted by several different cell types, four of which are mostly responsible for the neural system operation (Zeisel et al. 2015).

Neuron is the cell type intrinsically responsible for signals transmission accross the neural network, being supported by other cell types, which provide neurons a healthy and favorable environment. Neurons are supported by oligodentrocytes in electrical signals transmission. Oligodendrocytes are responsible for neurons axon mielinization, which accelerates signal transmission accross the neural network. They also have been observed to support neurons metabolism (Philips and Rothstein 2017). Astrocytes are responsable for projecting their cytosol both around neuron axons and vascular vessels, supporting neurons to access nutrients and eliminate metabolites (Vasile, Dossi, and Rouach 2017). Microglia is a phagocytic cell, which is responsible for protecting the CNS from external pathogenic threats (Wolf, Boddeke, and Kettenmann 2017). These three main cell types, together with others, such as ependymal cells, Schwann cells and others, are called glia cells.

However, the occurrence of a tumor inside the CNS may threaten the harmony developed by these four cell types and disturb neurological functions. Tumors inside the CNS arise upon malignant transformation of CNS cells, most often astrocytes, oligodentrocytes and stem cells (Ohgaki and Kleihues 2005).

Gliomas are the most common tumor developed in the CNS, arising in a multistep process, which involves sequential and cumulative genetic and epigenetic alterations resulting from intrinsic and environmental factors (Omuro and DeAngelis 2013). Moreover, other tumors may also occur, such as meningiomas, medulloblastoma, pineocytoma and others.

Gliomas are classified by the World Health Organization (WHO) into four histological grades, according to their degree of undifferentiation, anaplasia and aggressiveness (Louis et al. 2016). Grade I is characterized by low proliferative potential, high probability of cure upon surgical resection and rare evolution towards higher grades tumors. Grade II also has low proliferative activity, however, it is characterized by high invasiveness and usual recurrence after surgical resection. Grade III gliomas display nuclear atypia and elevated mitotic levels. Grade IV is assigned to cytologically malignant, mitotically active, necrosis-prone neoplasms, being usually associated to a fatal outcome. Examples of grade IV neoplasms include glioblastoma, most embryonal neoplasms and many sarcomas. They are mainly characterized by widespread infiltration and propensity for cranialspinal dissemination (Louis et al. 2007).

Glioblastoma accounts for the majority (55.1%) of gliomas, being the most common of all malignant CNS tumors (46.1%). While 94.2% of patients with pilocytic astrocytoma (Grade I) reach five-years survival post diagnosis, this percentage decreases to 5.1% for glioblastoma patients. The incidence of glioblastoma increases with age, the highest rates occurring in the 75 to 84 years, being 1.6-fold higher in males and 2-fold higher in caucasians as compared to African descendents (Ostrom et al. 2015).

Glioblastoma was also called glioblastoma multiforme, a name which was proposed and used for a long time because cells in these tumors vary in size and shape, but this term is no longer in use.

According to the last WHO CNS tumors classification, the median overall survival for glioblastoma patients after surgery, chemotherapy and radiotherapy is 15 months. In 10% of the glioblastoma cases, isocitrate dehydrogenase (IDH) is mutated conferring a significatively higher life expectancy (31 months) (Louis et al. 2016).

Although IDH mutation has been related to a longer survival rate, it has also been proposed as being responsible for driving grade II and III gliomas into glioblastoma. Specific point mutations in isocitrate dehydrogenase 1 and 2 (IDH1 and IDH2) inactivate wild-type enzymatic activity and convey a neomorphic function to yield D-2-hydroxyglutarate (D-2HG), which accumulates at millimolar levels within tumors. D-2HG can impact α-ketoglutarate-dependent dioxygenase activity and subsequently affect various cellular functions in these cancers (Parker and Metallo 2015). Other important genes for tumorigenesis, such as TERT, TP53, ATRX, EGFR and PTEN, were also found to be mutated in glioblastomas, but none of them displays clinical implications as important as IDH (Louis et al. 2016).

Gliomas were previously classified according to genomic alterations by Verhaak and collaborators (2010) into four groups (classical, proneural, neural and mesenchymal), but no clear correspondence was found with the WHO classification, survival rates and therapeutical approaches.

The current glioblastoma therapeutical approach is maximum tumor resection, followed by radiation therapy and chemotherapy with temozolomide. Temozolomide, an imidazotetrazine derivative of dacarbazine, is an oral alkylating agent which has relevant penetration into the central nervous system. It has 96-100% bioavailability and promotes methylation of the guanine O^6 position (N7-guanine and N3 adenine). It was approved in 1999 for usage to combat malignant gliomas. Major toxicities include nausea and myelosuppression (often low platelet counts) (Alifieris and Trafalis 2015). Considering the short survival after diagnosis under the current treatment scheme, it is imperative to seek for new approaches to develop new and effective therapies for glioblastoma.

A previous study from our group revealed that overexpression of Ectodermal-neural Cortex 1 (ENC 1) in rat C6/ST1 glioma cells resulted in significant reduction of the tumorigenic potential (Degaki, Demasi, and Sogayar 2009). However, little is known about ENC1 in human tumors, especially regarding its clinical relevance. The first chapter of this thesis evaluated ENC1 tumor suppressing properties in human glioblastoma cells, analysed ENC1 expression during human glioma progression and correlated ENC1 expression levels to patient prognosis.

In addition, this work also aimed at the development of a new approach for glioblastoma therapeutics. Because of the difficulty to completely remove gliomas by surgical resection, radiation and chemotherapy play a vital role in treatment of these tumors. However, the effect of chemotherapy still remains unsatisfactory, due to several limitations of the commonly used chemotherapeutic agents, such as systemic cytotoxic effects and limited drug penetration, which is attributed to both the blood−brain barrier and the blood−tumor barrier (Shi et al. 2015). Using the Phage Display methodology, the

second chapter describes the identification of a human glioblastoma-penetrating peptide, which may be used in further studies of targeted drug delivery therapeutics.

The Phage Display technology was developed by George Smith, from the University of Missouri, who inserted foreign DNA fragments into gene III of the M13 filamentous bacteriophage, to create a fusion protein containing the foreign sequence (G. P. Smith 1985). The fusion protein was incorporated into the virion, which retained infectivity and displayed the foreign aminoacids sequence in an accessible form. Combinatorial peptides, encoded by degenerate oligonucleotides, can be expressed at the N-terminus of the major (i.e. 2,500 copies) or minor (i.e. five copies) capsid proteins – pVIII or pIII, respectively – of bacteriophage M13 (Kay, Kurakin, and Hyde-DeRuyscher 1998). Among several applications, Phage Display is a powerful tool for identification of cell-penetrating peptides.

Peptides and proteins internalized by cells have been the subject of intensive study in recent years, since translocation across the cell membrane is critical for drug delivery and gene therapy. Significantly, the advent of Phage Display has provided a powerful technique to confer this property to bacteriophage and, in the *in vitro* process, to select for peptides or proteins which facilitate cell penetration, probably by triggering receptor-mediated endocytosis (Gao et al. 2002).

The linkage between a polypeptide sequence expressed on the bacteriophage surface and the DNA encoding that sequence allows the identification of the peptide and facilitates rapid screening and identification of polypeptides with novel and desirable properties. Since this method was developed, Phage Display has matured as a widespread technology for harnessing the chemical and structural diversity of peptide

and protein libraries and has revolutionized the discovery of molecules for many endeavors in academia and industry (Gao et al. 2002).

Additionally, during the development of this thesis, the author was extensively trained in cytometric techniques, which allowed him to conceive a side-project aimed at the development of a fluorescence-based method to generate cell growth curves for adherent cell cultures. The third chapter of this thesis describes this new method, which is based on staining the cells with carboxyfluorescein diacetate succinimidyl ester (CFSE) and monitoring the CFSE signal decay upon cell proliferation.

2. Upregulation of tumor suppressor Ectodermal-neural cortex 1 protein (ENC1) during human glioma progression is associated with unfavorable patient prognosis.

2.1. Introduction

Gliomas are the most common form of primary intracranial malignancy. In terms of etiology, gliomas most frequent arise from malignant astrocytes (astrocytomas), but they can also arise from oligodentrocytes, ependymal cells and neural progenitor cells. In terms of aggressiveness, the World Health Organization (WHO) classifies gliomas into grades I through IV. Grade IV (Glioblastomas – GBM) display the worst prognosis (15 months maximum life expectancy after diagnosis)(Sonabend, Ulasov, and Lesniak 2007; Louis et al. 2007), while grade I gliomas display a much favorable prognosis. Unfortunately, GBM is the most frequent type of glioma.

Ectodermal-cortex protein 1 (ENC 1), also known as Nuclear Restricted Protein/Brain (NRP/B), was first characterized as a protein which interacts with the cytoskeleton by binding to actin through Kelch-like domains, being related to neural fate specification during development of the nervous system (Hernandez et al. 1997). No ENC1 expression is found in normal astrocytes and oligodendrocytes (T. A. Kim et al. 1998; Y. Zhang et al. 2015), however, high expression levels of this gene are found in human glioblastoma (hGBM) (Liang et al. 2004).

ENC1 is a member of the Kelch superfamily, which consists of a large number of structurally and functionally diverse proteins characterized by the presence of one or

more Kelch-repeat domains. Kelch family members are involved in a number of cellular and molecular processes such as cell migration, cytoskeleton organization, regulation of cell morphology, protein degradation, and modulation of gene expression (Gupta and Beggs 2014). In addition to Kelch-like domains, ENC1 displays a BTB/POZ-like domain in the N-terminal. This domain has been proposed to mediate protein–protein interactions associated with higher order structures involved in chromatin folding and cytoskeleton organization (T. A. Kim et al. 1998).

Some studies have indicated that ENC1 displays tumor suppression properties (Polyak et al. 1997; Choi et al. 2014; Degaki, Demasi, and Sogayar 2009). In this context, p53 has been observed to upregulate ENC1 expression by transcriptional regulation (Polyak et al. 1997) and to inhibit cell proliferation by inhibiting E2F-target genes (Choi et al. 2014). Additionally, previous results from our group demonstrated that overexpression of ENC1 mediated the reduction of tumorigenic properties of rat C6 glioma cells (Degaki, Demasi, and Sogayar 2009). On the other hand, ENC1 has also been reported to promote tumor progression in ovarian cancer (Fan et al. 2018) and colorectal carcinoma (Fujita et al. 2001). To our knowledge, ENC1 expression levels during human glioma progression is yet to be addressed. Here, we confirmed ENC1 tumor suppression properties using a genomic random edition approach, analysed ENC1 expression in a set of patient glioma samples and correlated these data with patients survival and disease progression-free survival, concluding that ENC1 expression constitutes a biomarker for glioma aggressiveness.

2.2. Materials and Methods

2.2.1. Cell culture

The U87MG human glioblastoma cell line was cultured in low glucose Dulbecco's modified Eagle's medium (DMEM) containing 10% fetal bovine serum (FBS) and antibiotics (25µg/mL ampicillin and 100µg/mL streptomycin), incubated at 37°C in a humidified atmosphere containing 95% air/5% CO_2.

2.2.2. Generation of ENC1-edited U87MG cell line

Target sites for the ENC1 N-terminal were screened using the CRISPR Design platform (http://crispr.mit.edu). The small guide RNA (sgRNA) 5' TTGACTATGCGTACTCCTCC 3' was indicated as the lowest scored for off-targets probability, being chosen to be cloned into the pSpCas9(BB)-2A-GFP vector (pX458; Addgene; #48138). Cloning was carried out according to vector manufacturer´s instructions and insertion of the sgRNA was confirmed by Sanger sequencing. The U87MG human glioblastoma cells were transfected with this construct using Lipofectamine, according to the manufacturer´s instructions. After 48h, eGFP-positive cells were sorted using the FACS Aria II Cell Sorter (BD Biosciences).

2.2.3. T7 endonuclease assay

The ENC1 coding sequence was amplified by end-point PCR using genomic DNA (gDNA) isolated from eGFP-positive sorted cells as template (F-

ATGTCAGTCAGTGTGCATGAGAACC and R- TTAAGAAGGCAGATGTTTCC). The amplified fragment was denatured by heating at 95°C for 5min and the heteroduplexes were formed by cooling down to 85°C at 2°C/sec and then to 25°C at 0.1°C/sec. T7 endonuclease I digestion was carried out at 37° for 15min using 5U of T7 endonuclease I (T7E1; New England BioLabs) in a final volume of 10µL. The reaction was stopped by adding 1µL of 0.25 M EDTA. The digested heteroduplex was resolved in 1% agarose gel.

2.2.4. Characterization of ENC1 random editions by Sanger sequencing

The ENC1 coding sequence was amplified by end-point PCR using gDNA isolated from eGFP-positive sorted cells as template (F-ATGTCAGTCAGTGTGCATGAGAACC and R- TTAAGAAGGCAGATGTTTCC). The amplicon was purified, cloned into the pGEM-T Easy (Promega; #A3600) according to manufacture´s instructions and transformed into competent XL1blue *E. coli* bacteria. Colonies were ressuspended in 20µL of Luria-Bertani medium and 2uL of this bacterial suspension was used in conventional PCR, with the same primers used to amplify ENC1 from sorted U87MG gDNA. The PCR reaction was 10-fold diluted and used as template for Sanger sequencing with the R – CACAAGCCTTTCATCCTCTGTCT primer.

2.2.5. Clonogenic potential assay

Cells were sequentially diluted and $2x10^2$ cells were seeded onto 35mm plates in triplicate. Plates were incubated for 14 days in culture medium under a humidified atmosphere containing 5% CO_2, at 37°C. Cell colonies were then fixed in 3.7%

formaldehyde, stained with 1% crystal violet and manually counted.

2.2.6. Cell cycle assay

Cells were seeded in culture media onto 6-well plates ($5x10^4$ cells/well) in triplicate and incubated overnight under culture conditions. The culture medium was replaced by 0.5% FBS low glucose DMEM and cells were incubated for 72h. Cells were then harvested and fixed in cold 70% ethanol for 30 min, washed with PBS and stained for cell cycle analysis. Staining was carried out by incubation in staining medium (500µg/mL propidium iodide; 0.1% Triton-X and 1µg/µL RNAse A) at 4°C for 30min, followed by washing with PBS. Cells were analyzed in a FACS Aria II Cytometer (BD Biosciences) and propidium iodide fluorescence was detected using the PE-channel.

2.2.7. Cell growth curves

Cells were seeded in culture medium onto 12-well plates ($2x10^4$ cells/well) in duplicates and incubated overnight under culture conditions. The culture medium was replaced for 0.5% FBS low glucose DMEM and cells were harvested each 48h during 10 days. Cells were then immediately fixed in 3.7% paraformaldehyde and kept at 4°C. All samples were quantified together at the final of the experiment. The number of cells present at each time point was determined using the Accuri C6 Cytometer (BD Biosciences).

2.2.8. In vivo tumorigenic potential

Athymic BALB/c nude mice were randomly divided into two groups of four

animals each. The animals were maintained in a sterile environment. Cages, bedding and water were autoclaved, and animals were maintained on a daily 12h light/12h dark cycle. The protocols were approved by the Animal Ethics Committee (CEUA 030/16) and all the procedures were carried out according to the Brazilian Guidelines for Research Animals Handling (CONCEA). Cells were subcutaneously injected (1.0×10^6 cells/mouse) in 100µl of FBS-free low-glucose DMEM medium. Tumor dimensions were determined using a caliper, and the tumor volume was calculated as (the shortest diameter)×(the longest diameter)×(the shortest diameter x 0.5) at the following time points: 7, 14, 21, 28 and 31 days.

2.2.9. Analysis of ENC1 expression in patient glioma samples

RNA samples isolated from 75 human astrocytoma tumor samples were obtained from the Human Brain Bank of the Department of Pathology, School of Medicine of the University of São Paulo. Written informed consent for research purposes was obtained and the Ethical Research Committee of the University of São Paulo, Brazil, approved the procedure (CAPPesq 681/05; CONEP 830/01). The samples were from grade I astrocytoma (15 samples), grade II astrocytoma (15 samples), grade III astrocytoma (15 samples) and grade IV astrocytoma/glioblastoma (30 samples). A sample (2µg) of total RNA was used for cDNA synthesis using Super Script III (Life Technologies). ENC1 expression levels were analyzed using the ViiA 7 Real Time PCR equipment (Applied Biosystems, Brazil). The specific primers for ENC1 amplification were F - TGGAAACATCTGCCTTCTTAAATG and R – GGCCTCTCCGAAGTAGAAATCTC, and the housekeeping genes were HPRT (F – TTTGTTGTAGGATATGCCCTTGACT and R

– CTCAACTTGAACTCTCATCTTAGGCTTTGT) and GAPDH (F – ACCCACTCCTCCACCTTTGA and R – CTGTTGCTGTAGCCAAATTCGT). The results were calculated using the ΔCt method (Pfaffl 2001).

2.2.10. Public data in silico analysis

The *in silico* analysis was carried out using the R2: Genomics Analysis and Visualization Platform (https://hgserver1.amc.nl/cgi-bin/r2/main.cgi). ENC1 expression in different glioma grades was assessed using the public database “Tumor Glioma – French – 284 – MAS5.0 – u133p2” and the analysis of patient overall survival and disease progression-free survival was based on the “Tumor Glioblastoma – TCGA – 540 – MAS5.0 – u133a” database. For survival curves, we considered the median of ENC1 expression as the cut-off for patient segregation into high e low expression.

2.3. Results

Previous studies have addressed ENC1 functional properties by gain and loss of function mediated by lentiviral overexpression and interference RNA approaches (Polyak et al. 1997; T. A. Kim et al. 1998; Choi et al. 2014). Alternatively, in this work, we decided to address the ENC1 functional analysis of human glioma using the CRISPR/Cas9 genomic edition. U87-MG human glioblastoma cell line was used to generate a population of ENC1 gene edited cells. The sgRNA was designed to target the ENC1 N-terminal (Figure 1A). Transfected cells were sorted based on GFP expression by flow cytometry (Figure 1B). Cas9-mediated double strand breaks triggered error-prone DNA repair, leading to random insertions and deletions in the ENC1 coding sequence, abrogating ENC1 expression due to changes in the mRNA frameshift. The edition was confirmed by the endonuclease assay (Figure 1C). The presence of two distinct bans in the transfected cell sample revealed the presence of genomic edition. Considering the off-target sites listed by the CRISPR Design platform, the most likely site (chr3:+64037846) was screened for off-target edition by the endonuclease assay, and no off-target edition was observed, as shown by the presence of a single band in agarose gel (Figure 1D). Finally, the ENC1 coding sequence was screened to characterize in more details the genomic edition resulted from CRISPR/Cas9 activity, confirming the presence of random insertions and deletions in targeted region (Figure 1E).

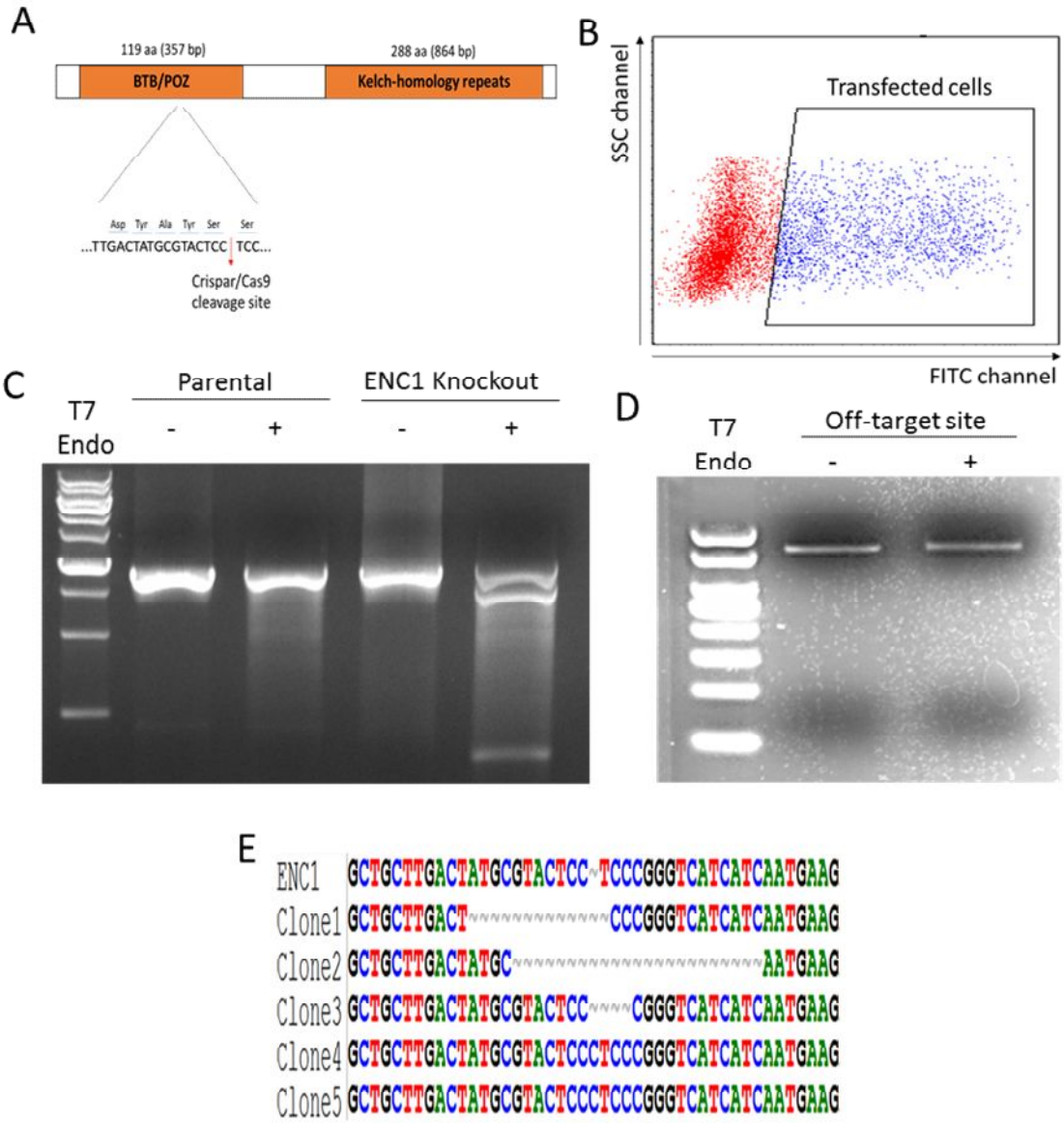

Figure 1. Generation and characterization of ENC1 edited U87MG cells. (A) An ENC1 N-terminal targeted sgRNA was cloned into the pX458 CRISPR/Cas9 vector and transfected into U87MG cells. (B) Sorting of transfected cells (48h post-transfection) according to the eGFP reporter protein from pX458 vector. (C) Endonuclease assay on ENC1 coding sequence amplified from transfected and non-transfected cells. (D) Endonuclease assay on the most probable site for off-target edition (chr3:+64037846) according to the CRISPR design software (www.crispr.mit.edu). (E) Analysis of ENC1 coding sequence amplified from transfected cells.

The tumorigenic properties of U87MG-edited cells was compared to the wild type cell line. ENC1 random editions increased the clonogenic potential of U87MG cells

(Figures 2A and B; 23 parental colonies versus 47 ENC1 knockout colonies), decreased the percentage of cells in G1-phase of cell cycle (Figures 2C and D; 82% parental cells versus 68% ENC1 knockout cells), increased the *in vitro* proliferative properties of U87MG cells (Figure 2E; 400,717 parental cells versus 731,992 ENC1 knockout cells at time point 240h) and, accordingly, increased the *in vivo* tumorigenic potential of U87MG cells to grow as subcutaneous tumors in Balb/c nude mice (Figure 2F; 549 mm^3 parental cells versus 1154 mm^3 ENC1 knockout cells – tumor volume 31 days after inoculation). Taken together, these data obtained by a new approach (ENC1 genomic random edition) confirms the previous findings regarding ENC1 as a protein with tumor suppression properties.

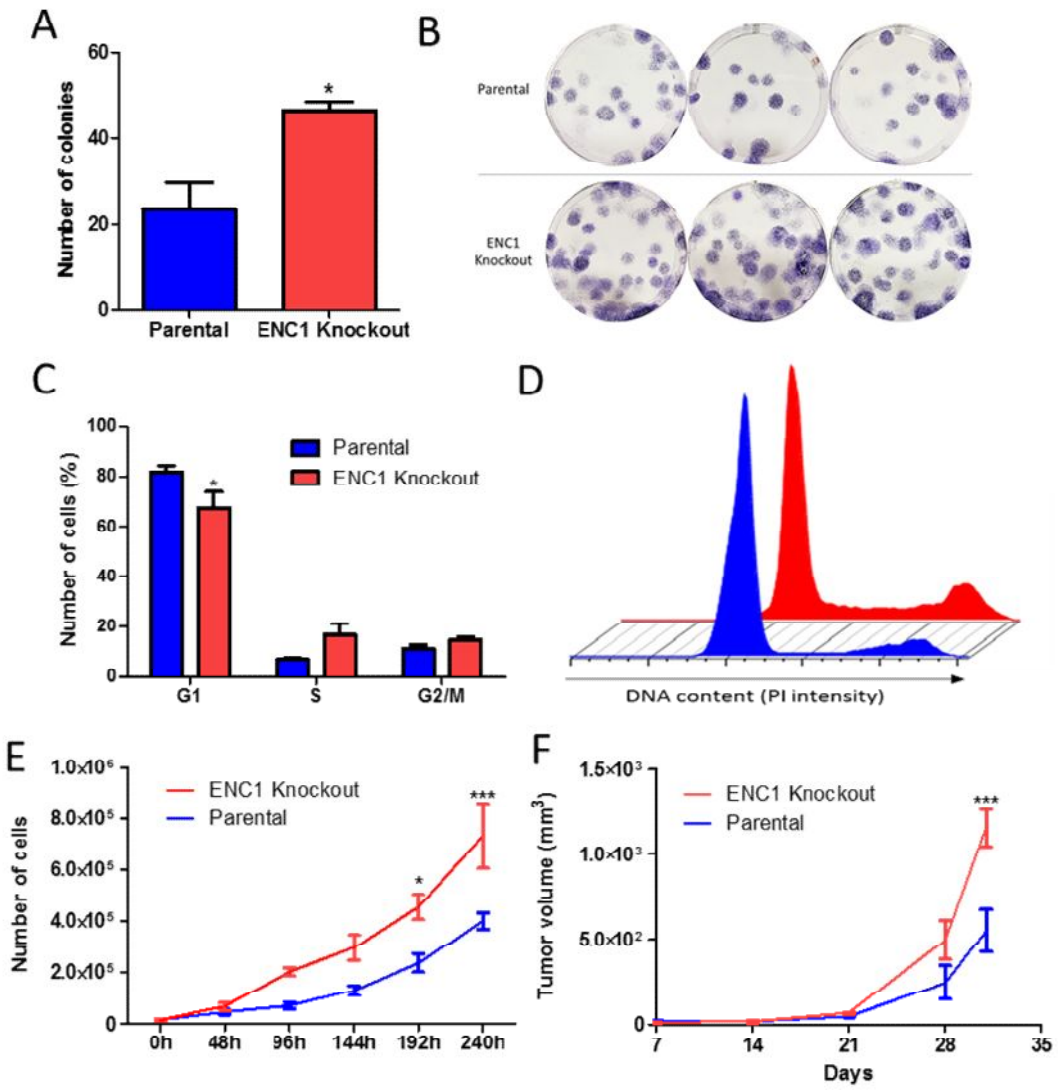

Figure 2. Functional analysis of ENC1 random edition U87MG cells. (A) Clonogenic potential of ENC1 knockout U87MG cells. Results are shown as the mean ± SEM of four independent experiments. * $p<0.05$ by paired T test. (B) Representative image of clonogenic assays. (C) Cell cycle analysis of ENC1 knockout U87MG cells. Results are shown as the mean ± SEM of three independent experiments. * $p<0.05$ by two-way ANOVA test. (D) Representative DNA content plot from cell cycle analysis. (E) Growth curve of ENC1 knockout U87MG cells. Results are shown as the mean ± SEM of three independent experiments. * $p<0.05$ and *** $p<0.001$ by two-way ANOVA test. (F) *In vivo* tumorigenic assay. Tumors were measured at 7, 14, 21, 28 and 31 days. Four animals were injected with each cell line. Results are shown as the mean ± SEM of two independent experiments. *** $p<0.001$ by two-way ANOVA test.

Next, we used a tumor panel of 75 glioma patients to investigate how ENC1 expression is modulated during glioma progression. This panel comprised samples of

pilocytic astrocytoma (glioma grade I), glioma grade II, glioma grade III and glioblastoma (glioma grade IV; Figure 3A), according to the World Health Organization classification of tumors of the Central Nervous System (Louis et al. 2016). Pilocytic astrocytomas usually have a circumscribed growth pattern, lack IDH gene family alterations and frequently display BRAF alterations. In addition, patients bearing this tumor type have good prognosis, being considered to be cured after tumor resection. Compared to pilocytic astrocytomas, tumor diffusiveness properties are strikingly increased in grades II to IV, also known as diffuse gliomas (Louis et al. 2016). As shown in figure 3B, diffuse gliomas express higher levels of ENC1, when compared to pilocytic astrocytomas. We addressed this same question using a public database of 284 glioma patents, with the same pattern being observed (Figure 3C).

A

	Pilocytic astrocytoma	Glioma Grade II	Glioma Grade III	Grade IV (GBM)
Cases	15	15	15	30
Mean Age	19y 8mo	34y 6mo	32y 10mo	53y 7mo
Gender				
Male	7	10	9	23
Female	8	5	6	7
Ocurrence				
Primary	15	14	14	27
Recurrent	0	1	1	3
Survival status				
Live	15	11	10	1
Dead	0	4	5	29

Survival status according to the last follow up records

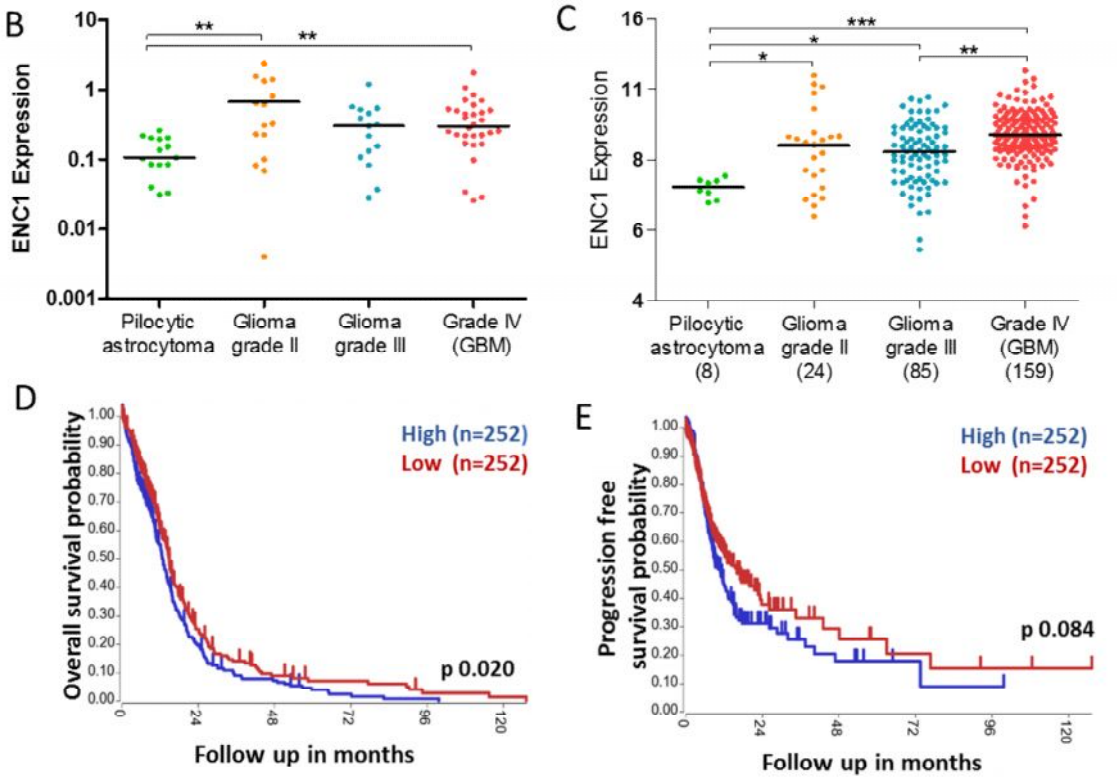

Figure 3. Analysis of ENC1 expression in different glioma grades and respective clinical relevance. (A and B) Assessment of ENC1 levels during glioma progression by qRT-PC using a cohort of 75 patients. GAPDH and HPRT were used as housekeeping genes. ** p<0.01 by one-way ANOVA test. (C) Assessment of ENC1 levels using a cohort of 276 patients from the "Tumor Glioma – French – 284 – MAS5.0 – u133p2" public dataset. * p<0.05, ** p<0.01 and *** p<0.001 by one-way ANOVA test. (D) Overall survival and (E) progression-free survival analysis in a cohort of 540 glioblastoma patients "Tumor Glioblastoma – TCGA – 540 – MAS5.0 – u133a". Curves were plotted using the R2: Genomics Analysis and Visualization Platform (https://hgserver1.amc.nl/cgi-bin/r2/main.cgi) using the median of expression values as the cut-off for patient segregation into high and low expression groups.

Considering the tumor suppressing properties of ENC1 (Figure 2), it is possible that upregulation of ENC1 expression occurs in an attempt to recover normal cellular proliferation rates. Therefore, we hypothesized that ENC1 levels could feature as a reporter for tumor aggressiveness, and approached this hypothesis by analyzing whether (or not) ENC1 levels are associated to patients survival. We used a public dataset of 540 glioblastoma samples to plot overall survival and disease progression-free survival curves as a function of ENC1 expression levels. As expected, according to our hypothesis, half of the patients with higher ENC1 expression displayed shorter overall survival and disease progression-free survival, in comparison to the lower expression half (Figures 3D and E).

2.4. Discussion

The Ectodermal-neural Cortex 1 (ENC1) gene, also called Nuclear Restricted Protein/Brain (NRP/B), was first identified in murine as being expressed during early gastrulation in the prospective neuro-ectodermal region of the epiblast (Hernandez et al. 1997), and, later on, the human orthologue was identified in neurons and observed to be absent in human astrocytes (Hernandez et al. 1998; T. A. Kim et al. 1998). However, aberrant ENC1 expression has been reported in gliomas originated from astrocytes (Liang et al. 2004; Hernandez et al. 1998) and tumors of different origins, such as human pituitary adenomas (Feng et al. 2014), colorectal carcinomas (Fujita et al. 2001), ovarian cancer (Fan et al. 2018), medulloblastoma (Yokota et al. 2004), breast cancer (Seng et al. 2007) and leukemia (Hammarsund et al. 2004).

The role of ENC1 in tumorigenesis is controversial in the scientific literature. ENC1 has been demonstrated to display tumor suppression properties in cervical carcinoma (Choi et al. 2014) and glioma (Degaki, Demasi, and Sogayar 2009; Liang et al. 2004; T.-A. Kim et al. 2000). The molecular mechanisms supporting this role involves upregulation of ENC1 expression by p53 (Polyak et al. 1997), the capacity of the ENC1 protein to bind to the hypo-phosphorylated form of the retinoblastoma protein (T. A. Kim et al. 1998) and its ability to act as a transcriptional reppressor of E2F-mediated transcriptional activity (Choi et al. 2014). On the other hand, other studies have observed that ENC1 promotes tumor progression in ovarian cancer (Fan et al. 2018) and colorectal carcinoma (Fujita et al. 2001). The molecular mechanism proposed by the authors were related to decreasing cellular ROS levels (Fan et al. 2018) and suppressing cellular differentiation (Fujita et al. 2001). Despite this controversy, little is

known about how ENC1 expression is modulated throughout glioma tumor progression and to what extent ENC1 expression is relevant to clinical aspects in patients.

In the present study, we first evaluated the influence of ENC1 expression in glioma tumorigenesis. Classical functional genomic analysis is based on gain and loss of function approaches. Although these approaches have been proposed to yield complementary information, gain of function experiments, mediated by gene overexpression, are known to be prone to artefact phenotypes (Moriya 2015; Ma et al. 2010). On the other hand, loss of function experiments are expected to deliver more functionally relevant results. In the ENC1 scientific literature, loss of function experiments have been carried out by targeting protein synthesis at the transcriptional level (knockdown), using interfering oligodesoxynucleotides (T. A. Kim et al. 1998), small interfering RNA (Fan et al. 2018) and short hairpin RNA (Choi et al. 2014). Considering the controversy in the literature, we set up to design a loss of function strategy based on different approach, by generating a CRISPR/Cas9-mediated ENC1 randomly edited U87MG cell line (Figure 1), confirming ENC1 tumor suppression properties in glioblastoma (Figure 2).

We next analyzed how ENC1 expression is modulated during glioma progression. Gliomas are classified into grades I trough IV by the World Health Organization (Louis et al. 2016; Louis et al. 2007). Grade I displays the best prognosis, while grade IV (glioblastoma) is the most aggressive and malignant lesion. We used a panel of 75 glioma patient samples to analyze how ENC1 expression is modulated during tumor progression. The expression of ENC1 was observed to be upregulated as glioma

aggressiveness increases, which was confirmed by a larger cohort of patients using public database (Figures 3A and B).

The occurrence of loss of function mutations in tumor suppressor genes has been reported as the main cause for tumor suppressors failure (Lee 2018; Greenblatt et al. 1994; Rosen and Pishvaian 2014). We investigated the mutational status of ENC1 using the Catalogue of Somatic Mutations in Cancer (COSMIC; https://cancer.sanger.ac.uk/cosmic), with no relevant incidence of mutations being identified for ENC1 in glioma patient samples (4 mutations in 1,863 samples; 0.21%). Upregulation of tumor suppressor genes during tumor progression has been suggested as an attempt to restore proliferative control (Huynh 2004) and has already been observed for other tumor suppression genes in different cancer types, such as p53 in gallbladder cancer (Ghosh et al. 2013), MyoD in medulloblastoma (Dey et al. 2013) and pRb2 in hepatocellular carcinoma (Huynh 2004).

After finding that ENC1 levels correlate with the degree of tumor aggressiveness, we analyzed whether this correlation would associate to patients prognosis. Using a public dataset of 540 glioma patients, we observed that half of the patients with higher ENC1 expression have statistically shorter overall survival (Figure 3D) and disease progression-free survival (Figure 3E). Accordingly, low expression of ENC1 has been associated to a favorable prognosis in ovarian cancer (Fan et al. 2018).

2.5. Conclusions

In conclusion, our studies on ENC1 and human glioma progression show that: (a) ENC1 displays tumor suppression properties in U87MG human glioma cell line; (b) ENC1 expression is upregulated during human glioma progression; (c) ENC1 expression may be used as a biomarker for glioblastoma patients prognosis.

3. Identification and *in vitro* characterization of a novel peptide internalized by human glioblastoma cells.

3.1. Introduction

Gliomas are the most common malignancy in the brain. Glioblastoma (GBM) represents 81% of all glioma cases (Ostrom et al. 2014) and shows the most aggressive phenotype with very poor average patient life expectancy (15 months) in 90% of the cases (Louis et al. 2016). The current first-line treatment for GBM is tumor resection, followed by adjuvant radiotherapy and chemotherapy, including the DNA alkylating agent temozolomide (Omuro and DeAngelis 2013). Proposed non-surgical options to tackle this malignancy include immunotherapy (Platten et al. 2016), targeted gene therapy (Oka et al. 2016), biotechnological devices (Chan et al. 2016), drug-carrying lipossomes (Wei et al. 2015) and nanopolymers (Zou et al. 2016). However, these pharmaceutical approaches fail to reach therapeutic concentrations within intracranial tumors but build their circulating concentration high enough to induce systemic adverse events (Lesniak and Brem 2004). The systemic cytotoxic effects and limited drug penetration arise from the blood−brain barrier and the blood−tumor barrier (Shi et al. 2015; Staquicini et al. 2011). Therefore, development of brain tumor therapy is constrained by the lack of alternative approaches for effective drug delivery to tumor cells.

Among targeted drug delivery approaches, peptides and proteins that can target and internalize into specific cell types represent a key avenue for the development of

novel treatment options (Zahid and Robbins 2015). In particular, the phage display technology has been extensively used and represents a powerful tool for identification of functional peptides in both normal and pathological conditions (Arap et al. 2004; Cardó-Vila et al. 2008; Zahid and Robbins 2012; Zahid and Robbins 2015; Kay, Kurakin, and Hyde-DeRuyscher 1998; Wu et al. 2016). The match between the displayed peptide and the corresponding DNA coding sequence permits fast identification of the peptide sequence, which provides a rapid screening platform for selection. Since its inception and subsequent improvements, (G. P. Smith 1985), phage display has become a widespread technology to explore the chemical and structural diversity of polypeptide combinations and their properties (Gao et al. 2002).

Using targeted peptides and proteins has enabled the development of therapeutic strategies based on tumor-targeted drug delivery. The delivered payloads include anti-tumor drugs, such as doxorubicin (L. Zhang et al. 2016) and paclitaxel (Liu et al. 2015), nucleic acids like iRNA (Wang et al. 2015; An et al. 2015), vectors for gene therapy (Hajitou et al. 2006), functional biomolecules, such as a pro-apoptotic peptides activated upon internalization (Ellerby et al. 1999; Pasqualini et al. 2015; Arap et al. 2004) and gene delivery hybrid systems, such as the adeno-associated virus/phage hybrid vector (AAVP) (Hajitou et al. 2006; Staquicini et al. 2011; T. L. Smith et al. 2016). However, despite past and recent efforts, options for glioma treatment still lack any approved target delivery therapy. We describe the identification and *in vitro* characterization of a novel peptide endowed with human glioma cells internalization properties, which may serve as an important tool to develop innovative targeted strategies in glioma therapeutics.

4. Materials and Methods

4.1.1. Cell culture

Human glioblastoma (hGBM) cell lines (A172, T98G, U251, LN229, LN308 and LN428) were cultured in Dulbecco Modified Eagle's Medium (DMEM) containing 10% fetal bovine serum (FBS) and antibiotics at 37°C in a humidified atmosphere of 95% air and 5% CO_2. U87MG cells were cultured in low glucose DMEM under the same conditions.

4.1.2. Biopanning

To minimize non-specific interactions, hGBM cells (U87MG, A172 and U251; $2x10^6$ cells) were first incubated for 1h at 37°C in 30% FBS DMEM followed by 2h incubation in 0.5% FBS DMEM containing $2x10^{11}$ TU of phage particles from the M13KE phage display library (NEB; E8120S). Cells were thoroughly washed five times with 5% BSA in PBS and once with TRIS/Glycine buffer (pH 2.2) to eliminate non-internalized phage clones. Cells were collected by trypsinization, washed with PBS and disrupted by freeze and thaw cycles followed by physical disruption with an insulin syringe (0,45 x 13mm). Recovered phage clones were amplified, purified and titrated. After three rounds of selection, the recovered phage clones were sequenced to reveal the selected and enriched peptide sequences.

4.1.3. Internalization assay

hGBM cells ($1x10^5$) were blocked in 30% FBS DMEM for 1h at 37°C before incubation with targeted phage ($1x10^9$ TU) in 2% FBS DMEM. Cells were thoroughly

washed five times with 5% BSA in PBS and once with TRIS/Glycine buffer (pH 2.2) to eliminate non-internalized phage particles. Cells were collected by trypsinization, washed with PBS and disrupted by freeze and thaw cycles followed by physical disruption. The cell lysates were incubated with host bacteria ER2738 for phage titration.

4.1.4. Phage binding assay

U87MG cells ($1x10^5$) were incubated with phage particles ($1x10^9$ TU) in 2% BSA DMEM on ice for 2h. Bound phage particles were quantified using the Biopanning and Rapid Analysis of Selective Interactive Ligands (BRASIL) method (Giordano et al. 2001)

4.1.5. Immunofluorescence microscopy

U87MG cells were plated onto 8-well slide chambers (Lab-Tek; $3x10^4$ cells/well), blocked for 1h at 37°C in 30% FBS DMEM and incubated overnight with phage ($1x10^9$ TU) in 2% FBS DMEM at 37°C. Cells were thoroughly washed with 5% BSA in PBS and TRIS/Glycine buffer (pH 2.2) followed by fixation in 4% paraformaldehyde and permeabilization in 0.2% Triton X-100 in PBS. Phage particles were immunostained with rabbit anti-Fd phage antibody (Sigma, 1:500 dilution) and Cy3-conjugated anti-rabbit secondary antibody (Jackson Laboratories, 1:300 dilution). Images were acquired using the Nikon Eclipse Ti2 fluorescence microscope, and images were analyzed using the NIS-Elements AR4.20.01 acquisition software.

4.1.6. Alanine scanning

Seven mutated clones were generated by site-directed mutagenesis. Each of the seven original amino acid residues of the LHTNELQ peptide sequence were individually replaced with alanine (A). Phage internalization assays were conducted as described previously. Primers used for site-directed mutagenesis were as follows:

L1A-F GGGCTTGTGCGCATACTAATGAGCTGCAGTGCGGGGCCGCTG;
L1A-RCGGCCCCGCACTGCAGCTCATTAGTATGCGCACAAGCCCCGT;
H2A-F GGGCTTGTCTTGCGACTAATGAGCTGCAGTGCGGGGCCGCTG;
H2A-R CGGCCCCGCACTGCAGCTCATTAGTCGCAAGACAAGCCCCGT;
T3A-F GGGCTTGTCTTCATGCGAATGAGCTGCAGTGCGGGGCCGCTG;
T3A-R CGGCCCCGCACTGCAGCTCATTCGCATGAAGACAAGCCCCGT;
N4A-F GGGCTTGTCTTCATACTGCGGAGCTGCAGTGCGGGGCCGCTG;
N4A-R CGGCCCCGCACTGCAGCTCCGCAGTATGAAGACAAGCCCCGT;
E5A-F GGGCTTGTCTTCATACTAATGCGCTGCAGTGCGGGGCCGCTG;
E5A-R CGGCCCCGCACTGCAGCGCATTAGTATGAAGACAAGCCCCGT;
L6A-F GGGCTTGTCTTCATACTAATGAGGCGCAGTGCGGGGCCGCTG;
L6A-R CGGCCCCGCACTGCGCCTCATTAGTATGAAGACAAGCCCCGT;
Q7A-F GGGCTTGTCTTCATACTAATGAGCTGGCGTGCGGGGCCGCTG;
Q7A-R CGGCCCCGCACGCCAGCTCATTAGTATGAAGACAAGCCCCGT.

4.1.7. Competition assay

Binding assays were performed as described previously in presence of increasing concentrations of the synthetic LHTNELQ cyclic peptide (CPC).

4.1.8. Statistical analysis

Experimental results were analyzed by ANOVA, unless otherwise specified.

4.2. Results

Our biopanning strategy was designed to enable the selection of internalizing peptides while minimizing the recovery of surface-bound particles (Figure 1A). The first round was performed with $2x10^{10}$ phage particles of a cyclic 7-mer M13 phage peptide display library (NEB; E8120S), which represents approximately 16-fold library coverage ($1.28x10^{9}$ possible sequences). The phage input in the second and third rounds were the same ($2x10^{10}$ TU).

Independent biopannings were performed on A172, U251 and U87MG cells. Phage particles recovered from the second and third rounds of selection were quantitated to determine enrichment of internalizing clones. Whereas selections on U251 and U87MG cells did not produce enriched peptides, we observed a 4.6 fold increase in the number of phage particles recovered from A172 cells (2,000 recovered phage in the first round and 9,200 in the second round), a result strongly suggesting selection of targeted internalizing peptides (Figure 1B). The peptides LHTNELQ, MAPDSRV, LAPKTKT and the peptide SHMEYPR (containing the enriched motif SHM) were highly enriched and therefore selected for further characterization (Figure 1C).

The LHTNELQ phage displayed a striking incidence among phage clones selected after three rounds of biopanning on A172 cells, covering 36% of sequenced clones (Figure 1B). The LHTNELQ phage showed an outstanding 37-fold higher level of internalization level compared to the insertless phage, while the MAPDSRV, LAPKTKT and SHMEYPR phage clones presented only 1,2-, 1,8- and 1,8-fold higher levels. Selecting the LHTNELQ phage was key for the observed recovery enrichment (4.6-fold) from the second to the third rounds of biopanning.

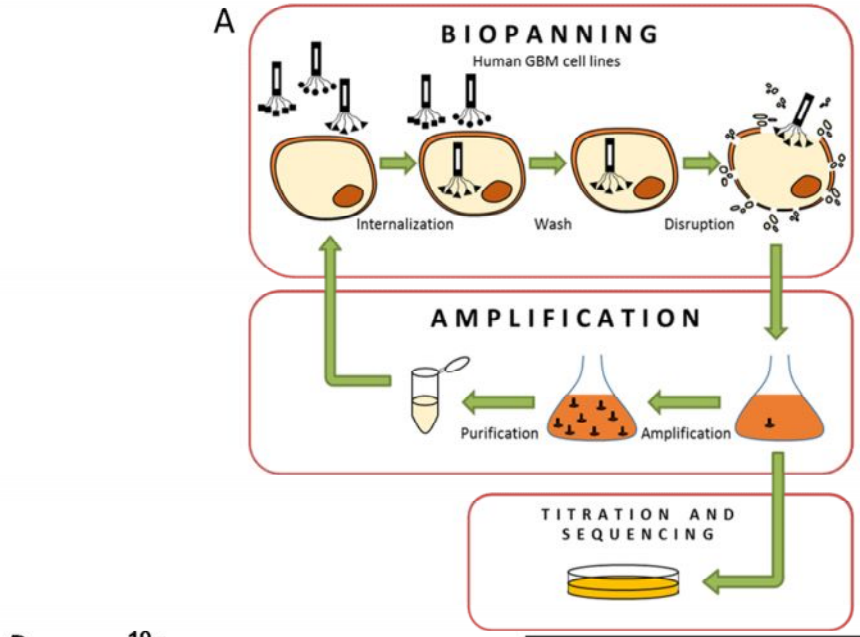

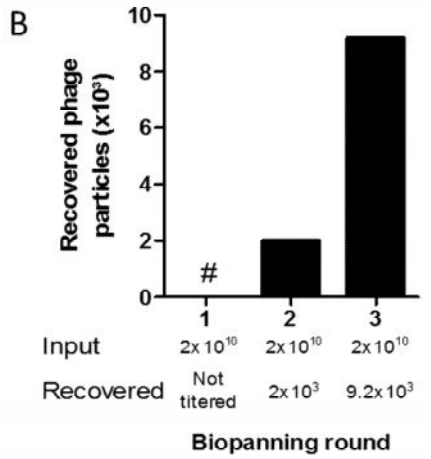

C

Peptide Sequence	Incidence	Peptide Sequence	Incidence
LHTNELQ	16/44	RGATPMS	2/44
MAPDSRV	6/44	NTASPYP	2/44
LAPKTKT	4/44	PLMVHGV	1/44
SHMEFSR	2/44	TVRTSAD	1/44
SHMEYSA	2/44	MPHNVSL	1/44
SHMEYPR	2/44	HQGLDTF	1/44
SHMEYSR	1/44	LAPKTKP	1/44
SHMGYPR	1/44	NPLSLSS	1/44

Figure 1. Selection of human glioblastoma internalizing peptides by *in vitro* biopanning. (A) Phage particles displaying cyclic random heptapeptide were incubated with hGBM cell lines. Biopanning was independently carried out on A172, U87MG and U251 cells. Cells were disrupted and internalized phage clones were recovered, amplified, purified, titered and used as input phage in two additional rounds. The input phage was the same during all rounds ($2x10^{10}$ TU). The phage output from the second and third rounds were titered in order to assess the recovery enrichment. The first round output was not titered to avoid losing unique clones. The third round phage output was sequenced to reveal the peptide sequences. (B) Enrichment of phage recovery from the second to the third round in biopanning on A172 cell. The number of phage particles recovered increased 4.6-fold, suggesting the selection of an internalizing clone. (C) Peptide sequence of 44 phage clones selected in the biopanning on A172 cells. The LHTNELQ sequence covered 36% of the sequencing output (16/44). The underlined sequence reveals a motif (SHME) which is present in different peptide sequences.

Internalization of the selected peptides was confirmed in A172 cells (Figure 2A; LHTNELQ internalization was 37-fold higher than insertless phage; MAPDSRV 1.2 fold; LAPKTKT 1.8 fold; SHMEYPR 1.8 fold). In particular, the peptide LHTNELQ showed an outstanding internalization compared to the others. When tested against several other hGBM cell lines, the peptide LHTNELQ showed specificity to A172 and U87MG cells (Figure 2B; LHTNELQ internalization in T98G cells – 262 phage particles; A172 – 3,564; U87MG – 4,063; LN229 – 175; LN308 – 150; LN428 - 88).

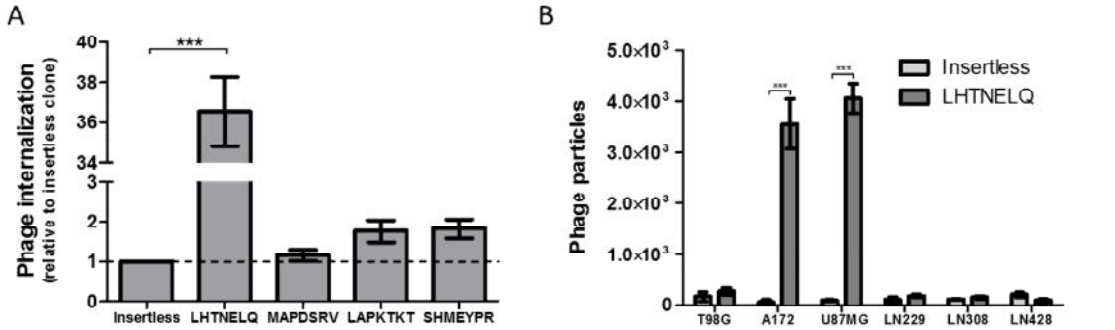

Figure 2. Screening of lead phage clones and analysis of the LHTNELQ phage internalization in different human glioblastoma cell lines. (A) Phage clones displaying the four lead peptide sequences, obtained by biopanning, were individually incubated for 2h with A172 cells. Cells were thoroughly washed and internalized phage was recovered by cell disruption. The LHTNELQ phage internalization was about 37-fold higher than the insertless phage. Results are shown after normalization as the mean ± SEM.*** $p<0.001$. (B) Screening of LHTNELQ phage internalization in different human glioblastoma cell lines. Phage incubation was carried out overnight. LHTNELQ was able to mediate phage internalization in A172 and U87MG cells. Results are shown as the mean ± SEM. *** $p<0.001$.

Next, we used the BRASIL method to assess binding of the peptide LHTNELQ to the surface of U87MG cells, and internalization after removal of unbound particles (Figure 3A; 3,592 insertless phage particles versus 33,486 LHTNELQ phage particles). We observed a 10-fold increase in the number of internalized LHTNELQ-phage compared to the control inserless phage (Figure 3B; 1,167 LHTNELQ phage particles recovered from non-disrupted cells versus 12,333 from disrupted cells), a result confirmed by immunofluorescence staining of internalized phage particles (Figure 3C). Internalization was also time-dependent, with no saturation observed up to 24h (Figure 3D; 525 internalized phage particles after 10min incubation; 1,050 after 30min; 2,650 after 1h; 6,300 after 4h; 30,467 after 8h and 86,667 after 24h). Additionaly, we used alanine scanning to investigate the individual contribution of each amino acid of the peptide LHTNELQ to its internalization and observed that binding and internalization are highly dependent on amino acids L1, T, N, E and L6. The amino acid H had no apparent contribution to peptide internalization (Figure 4; LHTNELQ - 100% internalization; AHTNELQ – 14%; LATNELQ – 91%; LHANELQ – 14%; LHTAELQ – 10%; LHTNALQ – 11%; LHTNEAQ – 11%; LHTNELA – 41%).

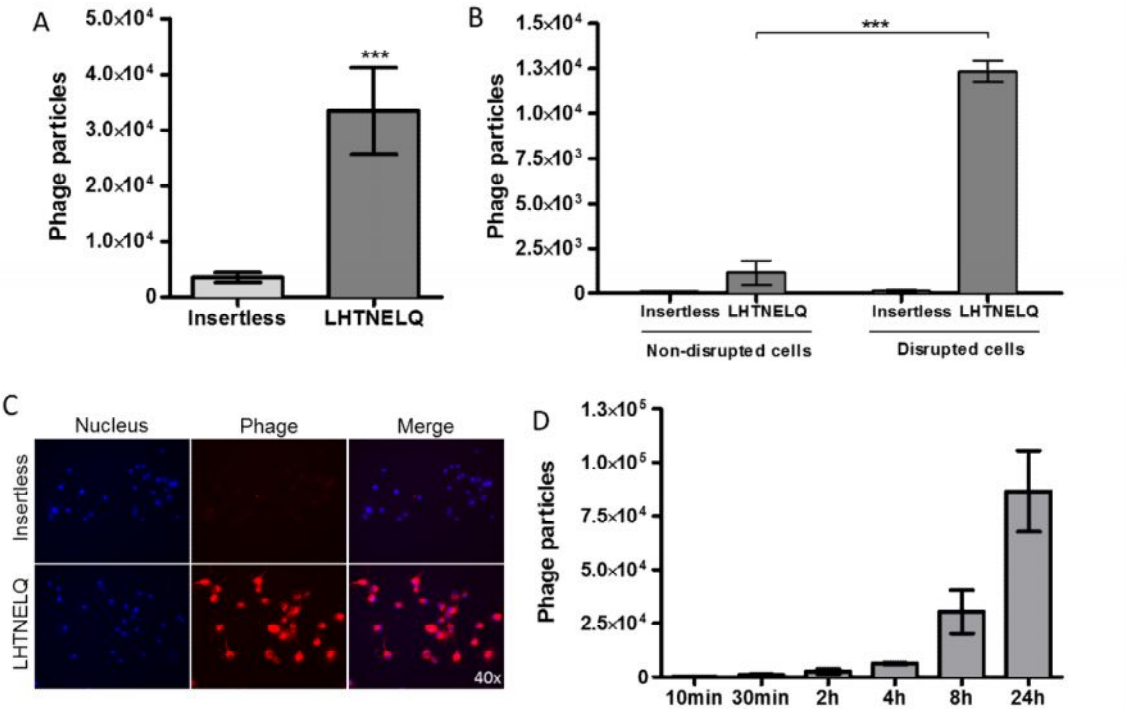

Figure 3. LHTNELQ phage binding and internalization properties in U87MG cells. (A) LHTNELQ phage binding was approached using the BRASIL assay. Phage was incubated with the cells for 2h in ice and unbound phage particles were then eliminated by centrifugation through an organic phase. Results are shown as the mean ± SEM. *** $p<0.001$ by paired T test. (B) LHTNELQ phage was incubated overnight with the cells. After washing, phage was recovered and titered from disrupted or non-disrupted cells. The number of recovered phage particles increased approximately 10.6-fold when cells were disrupted. Results are shown as the mean ± SEM. *** $p<0.001$ by two-way ANOVA followed by Bonferroni's test. (C) LHTNELQ phage was incubated overnight with the cells and phage internalization was addressed by anti-phage immunofluorescence. (D) LHTNELQ phage was incubated with the cells for different periods and cells were then washed and disrupted for phage recovery. The LHTNELQ phage is internalized in a time-dependent manner. No uptake saturation was observed in 24h.

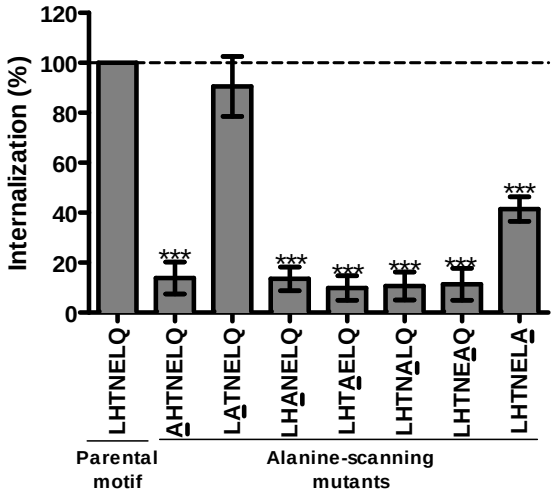

Figure 4. Screening of functional domain in LHTNELQ sequence. Each residue in the LQTNELQ sequence was mutated and the resulting phage clones were tested for internalization in U87MG cells upon overnight incubation. LHTNELQ phage internalization is independent of H2 residues and partially impaired by mutation of Q7. The other residues are essential for efficient internalization. Results are shown as the mean ± SEM. *** $p<0.001$.

Finally, because random mutations can occur in the phage genome during phage amplification to cause alterations in phage binding and internalization, we used the fUSE5 system to show that internalization induced by the peptide LHTNELQ is not dependent on the M13KE phage backbone (Figure 5A; Fd phage backbone 9.3 fold compared to the insertless phage; M13KE backbone 8.8 fold compared to the insertless phage). Moreover, the synthetic LHTNELQ cyclic peptide impaired LHTNELQ phage internalization, confirming that targeted phage internalization is dependent of displayed LHTNELQ peptide (Figure B; No peptide 100%; 50µg/mL synthetic peptide – 66%; 100µg/mL – 64% and 300µg/mL – 57%). Taken together, these results identify and characterize a peptide that is efficiently internalized into hGBM cells, and shows promise as a new tool for glioma therapeutic development.

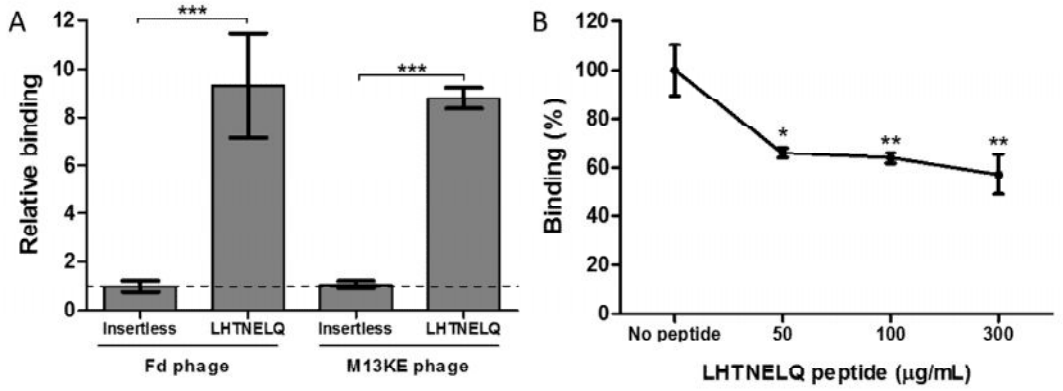

Figure 5 . Analysis of LHTNELQ-dependent phage internalization. (A) Cloning of the LHTNELQ coding sequence was carried out using both Fd and M13KE phage backbones. LHTNELQ mediated internalization was observed in both systems. Results are shown as the mean ± SEM. *** $p<0.001$ by paired T test. (B) Phage competition assays revealed that LHTNELQ phage internalization was decreased by cyclic LHTNELQ synthetic peptide, suggesting that the LHTNELQ domain mediates phage internalization by binding to an unknown cell surface protein. Results are shown as the mean ± SEM. * $p<0.05$ and ** $p<0.01$.

4.3. Discussion

Glioma-specific penetrating peptides represent a unique and promising alternative therapeutic approach to this deadly tumor. Since 2015, at least five clinical trials using targeted nanoparticles have been initiated, with the hope that this next generation of therapeutics will improve the lives of glioma patients. Here, we report the identification and characterization of the peptide LHTNELQ, a glioma-targeted peptide with robust internalizing properties of potential use for clinical applications.

Because internalization of the LHTNELQ-phage was partially inhibited by the synthetic corresponding peptide, we speculate that cell internalization is likely to occur due to binding to a cell surface receptor. Indeed, a BLAST search analysis suggested the peptide LHTNELQ may mimic binding partners of proteins highly present in brain cells, such as cullin-9 and nitric oxide synthase brain isoform. Nevertheless, several brain-internalizing peptides (such as angiopep-2 (Mei et al. 2014; Wang et al. 2015), Tat (Zheng et al. 2015), uPA-ACPP (B. Zhang et al. 2015), poly-arginine(Liu et al. 2016), LNP (Yao et al. 2015), T7 (Bi et al. 2016), Pen (Cates et al. 2016), RGD (Shi et al. 2015), iRGD (Sugahara et al. 2009) and iNGR (Alberici et al. 2013)) have been considered for drug development. Whether the new peptides described here will eventually serve as delivery vehicles to brain tumors remains an open question, and the objective of further investigation.

Saturation may occur due to low number of targeted cell surface proteins (receptor) or slow receptor turnover. The absence of saturation indicates that LHTNELQ mediated phage internalization efficiency. These results suggests that high phage concentrations can accumulate intracellularly over longer period of time. This important

feature of peptides reveals the utility of the candidate peptide for developing targeted drug-delivery strategies. (Figure 3D).

Competition assays usually result in a striking phage recovery abrogation after phage incubation with high concentrations of the synthetic peptide. However, we did not observe this in our assay, suggesting that the displayed peptide is more efficiently internalized than the synthetic peptide, even when the synthetic peptide is abundant. We conclude that a pentameric conformation of the peptides fused to the PIII may improve the efficiency of phage interaction with the receptor compared to the synthetic monomeric peptide. Based on this observation, we believe the use of PIII-displayed LHTNELQ peptide on adeno-associated virus/phage hybrid vector (AAVP) (Hajitou et al. 2006; Staquicini et al. 2011; T. L. Smith et al. 2016) may empower AAVP particles for an efficient targeted internalization in human gliomas. AAVP has shown to be very efficient to mediate coding sequences integration into cancer cells genome. However, targeting specificity and efficiency is crucial to avoid undesired gene integration events and we believe LHTNELQ displayed peptide may be an important tool for this purpose.

4.4. Conclusions

These results identify and characterize a peptide that is efficiently internalized into hGBM cells, and shows promise as a new tool for glioma therapeutic development.

5. Counting-free fluorescence-based method to generate growth curves of adherent cell cultures.

5.1. Introduction

In vitro cell culturing allowed the establishment of a number of cell lines from different organisms, developmental stages and disease samples. Currently, questions posed in several biomedical sciences fields may be answered using the outstanding platform of *in vitro* proliferating cells (Stacey 2012). Moreover, cell culturing may be used to produce recombinant molecules, since *in vitro* proliferating cells of different origins have been essential for the development of biopharmaceuticals in the Biotechnology industry (Kantardjieff and Zhou 2013; Marx 2012). The most classical tool to investigate *in vitro* cell proliferation is the cell growth curve.

Three steps may be described in cell growth curves, namely: Lag, Log and Stationary phases. The Lag phase is an adaptive step, with cell proliferation ensuing at increasing rates until cells reach the maximum proliferation rate, when the Log phase starts. During this phase, the number of cells grows exponentially and the growth rate is constant. Later on, the number of cells reaches saturation, the proliferation rate decreases, and the number of cells stop increasing as a consequence of limitations, such as: substrate exhaustion, product inhibition or growth inhibition by cell-to-cell contact, thereby defining the stationary phase (Freshney 2010). The cell growth curve is commonly plotted as the number of cells as a function of time, depicting a sigmoid curve from which it is possible to calculate the doubling time, also referred to as generation

time, expressing the period of time necessary for the number of cells to double, during the log phase, under specific culture conditions.

Different approaches may be used to assess cell proliferation *in vitro*. Incorporation of nucleoside-analogues, such as tritiated thymidine (^{3}H-TdR) and 5-Bromo-2′-deoxyuridine (BrdU), is used to identify cells which are in the S phase of the cell cycle. Proteins associated with the cell cycle, such as Ki-67, phosphorylated-histone H3 and proliferating cell nuclear antigen (PCNA), are also used as cell proliferation reporters. In addition, cytoplasmic proliferation dyes, such as carboxyfluorescein diacetate succinimidyl ester (CFSE) and the cell trace violet (ThermoFisher Scientific, Cambridge, MA) have been employed to track proliferating cells (Romar, Kupper, and Divito 2016).

CFSE is a cell-permeant non-fluorescent pro-dye. Once the molecule is inside the cell, its acetate group is cleaved by cellular esterases and the resulting green fluorescent carboxyfluorescein molecule is no longer membrane permeable, binding to free amine groups through the succinimidyl ester group, which generates covalent dye-protein conjugates. CFSE was employed, in 1994, as a cell tracker, to identify proliferating lymphocytes after a stimulus (Lyons and Parish 1994). When stimulated, lymphocytes proliferate, with each daughter cell receiving half the CFSE content present in the mother cell. CFSE has become a powerful tool in the Immunology field (Benjamin J C Quah and Parish 2012; Ben J C Quah, Warren, and Parish 2007; Rabah et al. 2001). Later on, CFSE was used to analyze the interference of drugs in cell lines proliferation (Chang et al. 2002; Rabah et al. 2001) and their doubling time (Chung et al. 2017).

Despite the fact that different technical approaches have been developed for cell proliferation analysis, the cell growth curve remains as a crucial tool to reveal the proliferative characteristic of cell cultures *in vitro,* such as the transition from Lag to Log and Stationary phases. The most classical approach to generate growth curves is by counting cells using the Neubauer chamber, however, this is quite laborious and variable, therefore, automated cell counters were introduced to facilitate and accelerate the cell counting process. Furthermore, some flow cytometers were adapted to count, in addition to analyzing cells. To the best of our knowledge, there are no alternative methods to generate adherent cells growth curves other than those based on absolute cell number determination. The accuracy in the conventional counting-based method is dependent on a precise determination of total number of cells, which is affected by disrupted cells, doublets and clumps formation and by cell loss during harvesting. Here, we propose a new method to plot growth curves, based on CFSE fluorescence signal, named counting-free florescence-based method (CFFM), which relies on following up the CFSE signal decay upon cell proliferation, being independent of total number of cells determination, thus eliminating the above mentioned interferences.

5.2. Materials and Methods

5.2.1. Cell culture

Human embryonic kidney cells (HEK 293 cell line, ATCC CLR-1573, Rockville, MD) were cultured in Dulbecco's modified Eagle's medium (DMEM; Gibco, MD, USA) supplemented with 10% fetal bovine serum (FBS; Vitrocell, São Paulo, Brazil). Cells were cultured at 37°C under a humidified atmosphere containing 95% air/5% CO_2.

5.2.2. Cells staining with CFSE

Cells were labeled using the CellTrace™ CFSE Cell Proliferation Kit (Thermo Fisher Scientific, Waltham, MA, USA; C34554), according to the manufacturer's instructions, with a few modifications. Cells ($1x10^6$) were washed with PBSA (PBS without calcium and magnesium), ressuspended in CFSE solution in PBSA (5µM CFSE – 1 mL final volume) and incubated for 20min at 37°C on a side-to-side shaker. A volume (9 mL) of 10% FBS DMEM was then added and the cells were incubated for 5min at 37°C in a side-to-side shaker in order to allow free CFSE to bind to serum proteins and improve free CFSE elimination. Labeled cells were centrifuged, ressuspended in 10% FBS DMEM and seeded for the growth curve experiment.

5.2.3. Growth curves

CFSE stained cells (5×10^4) were seeded onto 35mm wells in 10% FBS DMEM, with culture medium change every other day. Triplicate wells were harvested by trypsinization at the indicated time points and the cells were fixed in 1mL final volume of

3.7% formaldehyde. Growth curves were generated using four different approaches, namely: manual cell counting using the Neubauer Chamber, automatic cell counting using the Coulter Counter Analyzer (Beckman Coulter), automatic cell counting using the Accuri C6 Cytometer (BD Biosciences) and analysis of CFSE signal decay, also using the Accuri C6 Cytometer (BD Biosciences).

5.2.4. Manual cell counting using the Neubauer Chamber.

According to the manufacturer's instructions, a sample (10µL) of the cell suspension from each sample was loaded into the Neubauer chamber. The number of cells present in the four external quadrants of the chamber was counted and the mean was calculated and multiplied by 10^4 to yield the number of cells per milliliter. Highly concentrated samples were properly diluted to adjust the cell concentration to 10-100 cells per quadrant.

5.2.5. Automatic cell counting using the Z2 Coulter Counter Analyzer (Beckman Coulter)

The equipment was set to detect particles from 9 to 27µm and to take the sample dilution into account. An aliquot (100 µL) from each sample was diluted in PBS buffer and loaded into the equipment. The output values were delivered as the number of cells per milliliter.

5.2.6. Automatic cell counting using the Accuri C6 Cytometer (BD Biosciences)

An end point acquisition stop was set at 100µL for absolute cell counting. Cells were gated apart from debris in an SSC-A x FCS-A plot and the number of events were multiplied by 10 to yield the total number of cells per milliliter.

5.2.7. CFSE signal measurement using the Accuri C6 Cytometer (BD Biosciences)

Cells were gated apart from debris in a SSC-A x FCS-A plot. Single cells were then gated apart from the doublets and clumps in a FCS-H x FSC-A plot. An end point acquisition stop was set at 4,000 events inside the single cells gate, from which the CFSE median fluorescence intensity (MFI) was determined. The MFI values were plotted as a function of time to analyze the kinetics of CFSE decay. Next, the inverse of MFI (values were raised to the power of -1; MFI^{-1}) was plotted as a function of time in order to change the plot from descendent exponential into an ascendant exponential.

5.2.8. Doubling time calculation

The cell specific growth rate (µ) was determined from the slope of the natural logarithm of cell count or MFI^{-1} as a function of time and doubling time (DT) using the formula [$DT = \ln 2 / \mu$] (Castilho et al. 2008).

5.2.9. Statistical Analysis

Statistical analysis of the coefficient of variation of three replicates of the cell growth curves, determined by the different methods, was carried out by paired Wilcoxon tests. Analysis of CFSE MFI intensity and number of cells from time points 144h to

168h, in the presence or absence of 20µg/mL Mitomycin C, was carried out using the t test.

5.3. Results

The conventional method for generating growth curves of adherent cells is based on determination of the absolute number of cells at different time points, under specific culture conditions. Here, we compare this traditional approach to an alternative method, named counting-free fluorescence-based method (CFFM). This method is not based on determination of the absolute number of cells, but, rather, on following up the CFSE signal decay over time, depending on the analysis of only a small fraction of the total number of cells.

CFSE and other fluorescence cell tracers passively diffuse into the cells and covalently bind to cellular amine radicals. After cytokinesis, the daughter cells hold half the initial amount of CFSE stained amine radicals. Cell tracers (such as CFSE) allow monitoring cell proliferation from the exponential decay of the fluorescence signal, considering that, as cells proliferate, the CFSE content in each cell is split in half after each cell division (Figure 1A).

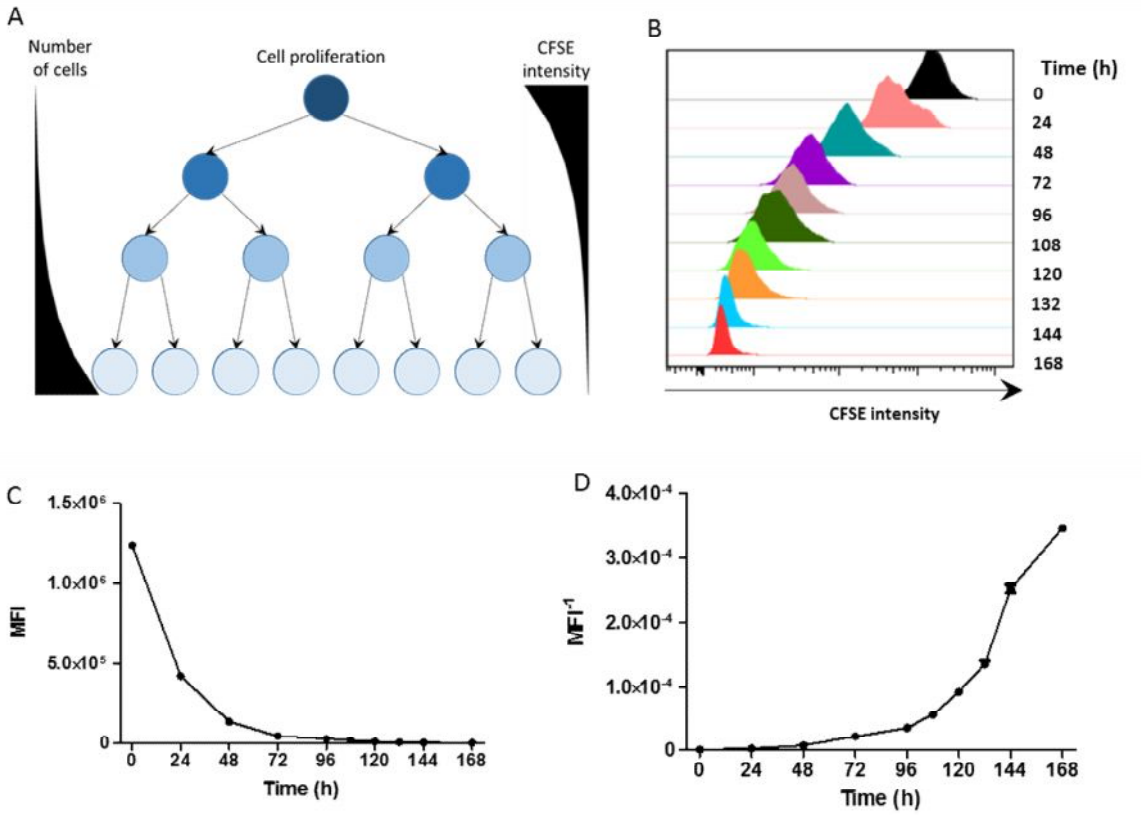

Figure 1. Analysis of CFSE signal decay upon cell proliferation. (A) CFSE passively diffuses into the cells and covalently binds to free amine residues. As cells divide, each daughter cell holds half of the CFSE content present in the mother cell. (B) HEK 293 cells were stained with CFSE and cultured for up to seven days. Cells were harvested and fixed at different time points and the CFSE fluorescence signal was measured. Consecutive cell divisions lead to progressive CFSE signal decay in the cell population. The experiment was carried out with three technical replicates. (C) CFSE MFI as function of time reveals the exponential CFSE signal decay. (D) The inverse of CFSE MFI values (MFI^{-1}) plotted as function of time renders the curve into a sigmoid, similar to the conventional growth curves.

HEK 293 cells were stained with CFSE, seeded onto several wells and cultured for seven days. Cells were harvested at different time points and the CFSE MFI was determined using the Accuri C6 Cytometer (BD Biosciences; Figure 1B). The CFSE MFI from each time point, plotted as a function of time, indicates that the signal exponentially decays as cells proliferate (Figure 1C). We hypothesized that CFSE MFI measurements could be mathematically treated to transform the descendent exponential plot into an

ascendant exponential plot, similarly to those obtained from conventional cell counting-based methods. Surprisingly, we observed that if we plot the inverse of the MFI values as a function of time, the exponential plot changed into an ascendant exponential, which fitted very closely the conventional cell growth curve (Figure 1D).

To compare with the CFFM curve, we used the same samples to determine the absolute number of cells using different types of equipment and plotted conventional growth curves. The conventional curves were plotted using three different counting devices, namely: the Neubauer chamber, the Coulter Counter Analyzer Cell Counter (Beckman Coulter) and the Accuri C6 Cell Counter (BD Biosciences). Interestingly, the curves profiles were very similar, indicating that the CFFM curve properly reveals cell proliferation dynamics (Figure 2).

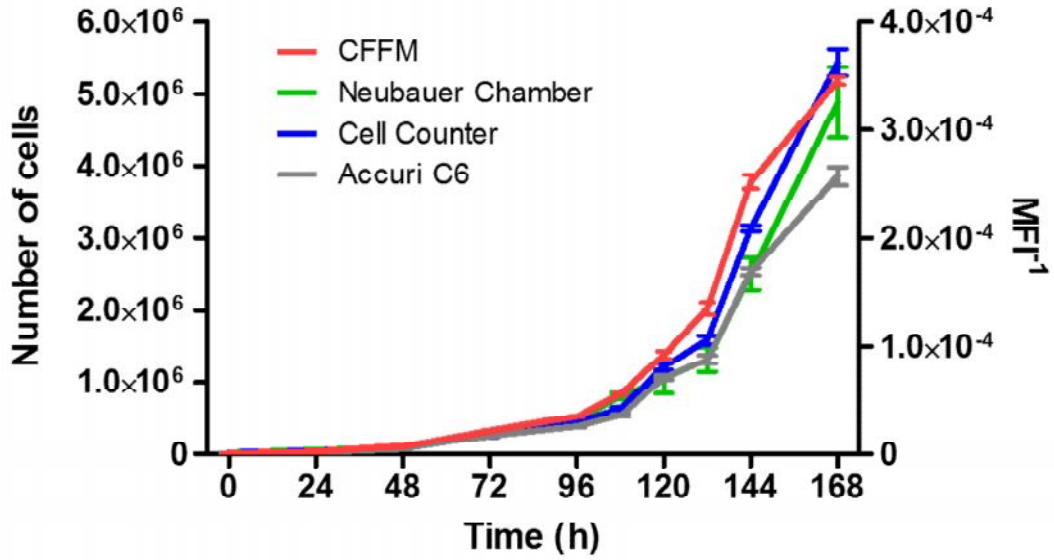

Figure 2. Comparison of HEK 293 growth curves plotted by counting-free fluorescence based method (CFFM) and counting-based methods. HEK 293 cells were stained with CFSE and cultured for up to seven days. Cells were harvested and fixed at different time points. The experiment was carried out with three technical replicates. The total number of cells (left Y axis) was determined at each time point using three different types of equipment, namely: Neubauer Chamber, Coulter Counter Analyser (Beckman Coulter) and Accuri C6 Cytometer (BD Biosciences). The CFSE MFI at each time point was determined using the Accuri C6 cytometer, and its inverse (MFI^{-1}) was plotted in the right Y axis.

We quantitatively analyzed the results obtained using the different counting methods by comparing the doubling time values obtained from each of the curves. As shown in Table 1, the CFFM yielded a doubling time slightly lower than those calculated from the conventional growth curve. As detailed below, we believe that this difference is due to the lack of interference of cell loss, cellular debris and cell clumps in the CFFM method, factors which influence the conventional methods.

Table 1. Doubling time comparison.

Method	Doubling time
CFFM	18h 56min
Neubauer Chamber	20h 41min
Cell Counter	20h 05min
Accuri C6	20h 16min

The accuracy of cell growth curves generated by cell counting-based methods depends on the precision of total number of cells determination. On the other hand, this is not a requirement for CFFM, which is not influenced by the number of cells analyzed. Apart from cellular debris and cell clumps, only single cells (4,000 events) were analyzed at each time point to generate the CFFM cell growth curve. As shown in Figure 3A, the single cells were gated apart from the doublets and cellular debris and MFI was calculated using 4,000 events within the single cell gate. Therefore, the main advantage of CFFM is to be resistant to technical interferences, which are otherwise unavoidable in counting-based methods. Here, we underline three drawbacks of the counting-based methods, which have no influence on CFFM (Figure 3B).

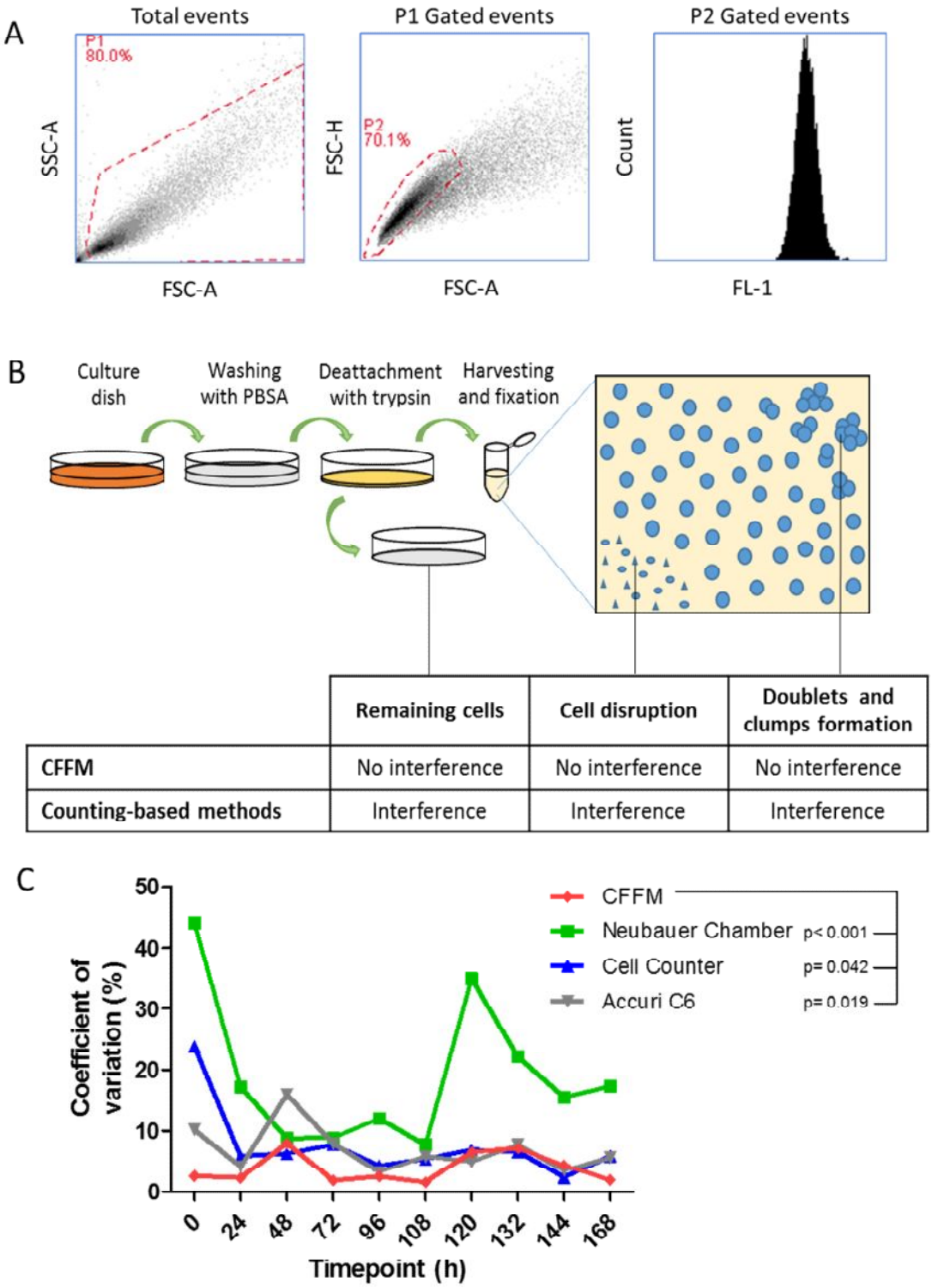

Figure 3. Variation among replicate measurements for each dataset. (A) Gating strategy for the determination of CFSE MFI for each time point. Cells were gated apart from debris in SSC-A x FCS-A plot. Considering only P1 gated events, single cells were gated apart from the doublets and clumps in FCS-H x FSC-A plot, and the CFSE MFI was measured considering only single

cells. The analysis considered 4,000 events into the single cells gate. (B) The presence of debris, doublet and clumps after cell harvesting and fixation interfere the final results of counting based methods, as well as those cells that remain in the plate after harvesting. On the other hand, these influences does not interfere on CFFM, which is based on the CFSE signal intensity of a small sample of single cells from each time point. (C) The coefficient of variation of three replicates for each time point. Statistical analysis was carried out by paired Wilcoxon test.

Firstly, the counting-based methods are influenced by cell loss during cell harvesting from the culture plate. Cell growth curves usually start with a few cells in the first time points and a much higher number of cells at the last time points, reflecting a comprehensive representation of cell proliferation dynamics. The coefficient of variation among the three replicates in the first time points, in the case of the counting based methods, is much greater than that of CFFM, because any cell loss during harvesting has a great influence, considering the low number of cells present at these first time points (Figure 3C). Losing cells during harvesting has no interference in the CFFM method, considering that a small sample of harvested cells is sufficient to address the CFSE MFI of single cells at any time point. Secondly, cells which are disrupted into cellular debris are not taken into consideration in the counting-based methods, since they are out of the range of detection, underestimating the total number of cells. Thirdly, whether or not the doublets and cell clumps are considered, the cell counting-based methods are biased towards underestimation of the total number of cells, especially in the last time points, when the cellular density is higher.

Therefore, elimination of these interferences enables the CFFM method to yield cell growth curves with lower variation among replicates when compared to the counting-based methods. This is quantitatively demonstrated by comparing the coefficient of variation of the triplicate measurements for each time point of the curve (Paired Wilcoxon test; Figure 3C).

Finally, we investigated the reliability of the CFSE signal decay as a consequence of cell proliferation in the two last time points (144 and 168 hours). Considering that at these time points the CFSE has been maintained at 37°C inside the cells for a long time, these time points were also chosen to address spontaneous CFSE degradation, which could mislead the representation of cellular proliferation dynamics. To address this question, the MFI of these last two time points was compared using Mitomycin C to halt cell proliferation. The number of cells did not increase upon Mitomycin C treatment and, in which case no CFSE signal decay was observed, confirming CFSE stability even after seven days under cell culture conditions (Figure 4).

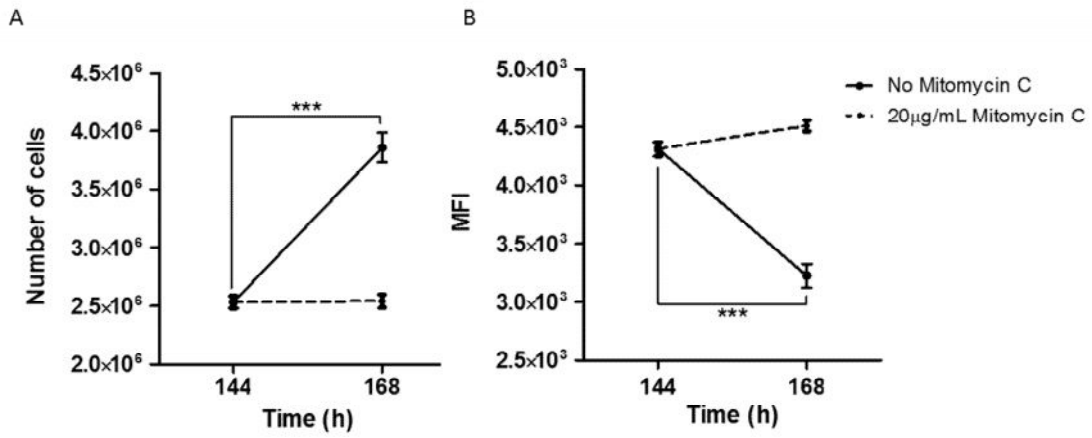

Figure 4. Analysis of CFSE stability in the last two time points of the cell growth curve. Cell proliferation was stopped at time point 144h using Mitomycin C to analyze proliferation-independent CFSE MFI decay. The experiment was carried out with three technical replicates. Statistical analysis was carried out by t test. (A) Mitomycin C treatment abrogates cell proliferation. (B) No CFSE MFI decay is observed in non-proliferating cells.

5.4. Discussion

CFSE was initially employed to analyze lymphocytes clonal proliferation upon stimuli (Lyons and Parish 1994). It is possible to detect different generations of proliferating clones, each of which may be identified in the plot as a peak, with different CFSE fluorescence intensity (Rabah et al. 2001; Ben J C Quah, Warren, and Parish 2007; Benjamin J C Quah and Parish 2012). The usage of CFSE to stain cell lines allows identification of a single peak, considering that all cells are proliferating with similar doubling time (Begum et al. 2013). As a result, the CFSE fluorescence intensity decreases as a function of time, allowing this methodology to be employed to assess cell proliferation under different conditions, such as genomic manipulations (Chang et al. 2002; Chaubey and Ghosh 2014), presence of nanopartical biomaterial (Goldman et al. 2015) and treatment with chemical compounds (Jiang et al. 2014). Moreover, the CFSE decay upon cell proliferation has been used to calculate cell lines doubling time (Chaubey and Ghosh 2014; Chung et al. 2017). In this context, to the best of our knowledge, this is the first time that CFSE is used to generate cell growth curves.

The growth curve plot is the most common analysis to characterize *in vitro* cultured cells. Growth curves determination of adherent cells constitutes a laborious task, in addition to be influenced by cell loss during cells harvesting, which directly affects the total number of harvested cells. Moreover, the presence of cellular debris and cell clumps increases the underestimation of total number of cells in cell-counting based growth curves. The CFFM method is an alternative approach to generate growth curves of adherent cells. The proof of concept that CFSE signal decay reflects cell proliferation

was demonstrated here by analyzing both proliferating and non-proliferating cells (Figure 4).

We also show that the CFFM method is not influenced by cell loss during cell harvesting, cellular debris or cell clumps, by comparing the growth curves obtained using different methods (Figure 2), highlighting the doubling time obtained from these curves (Table 1) and the variation among replicates measurements between CFFM and counting-based methods (Figure 3C).

The cell growth curve is an important reporter for changes in cellular functions under different conditions, such as drug treatments and functional genomic analysis. Development of accurate techniques to generate precise cell growth curves is important to provide reliability in determination of phenotypic changes which are dependent on identification of Lag, Log, and Stationary phase transitions. Moreover, determination of phase transitions is crucial for characterization of cell lines used for production of recombinant proteins in the Biotechnology Industry.

Furthermore, usage of cell tracers with different spectra to stain different cell lines allows the analysis of several cell lines simultaneously (Chung et al. 2017). Therefore, another advantage of CFFM is the possibility of simultaneously analyzing co-cultured cells. Counting-based methods do not allow the analysis of how two or more co-cultured cell lines modulate each other´s proliferation dynamics.

5.5. Conclusion

In conclusion, we described an alternative method for generating growth curves of adherent cells based on CFSE signal decay upon cell proliferation. This method displays lower variation among replicates when compared to that of cell counting-based methods, since it is not dependent on determination of the total number of cells at each time point, but, rather, on assessing the intensity of CFSE fluorescence of a small percentage of the total number of cells and, additionally is not influenced by cell loss, cellular debris or cell clumps.

Supplementary Table 1. Raw cell counts data using the Accuri C6 Cytometer (BD Biosciences).

Time (h)	Replicate 1	Replicate 2	Replicate 3	Mean	Standard Deviation	Coefficient of variation (%)
0	1,542	1,563	1,294	1,466.3	149.6	10.2
24	2,803	3,047	2,949	2,933.0	122.8	4.2
48	7,782	6,605	9,098	7,828.3	1,247.1	15.9
72	24,055	26,690	28,205	26,316.7	2,100.0	8.0
96	38,045	37,597	39,960	38,534.0	1,255.1	3.3
108	51,494	52,554	57,402	53,816.7	3,149.9	5.9
120	106,249	101,220	111,833	106,434.0	5,308.9	5.0
132	122,405	128,901	142,290	131,198.7	10,139.7	7.7
144	256,655	243,015	259,874	253,181.3	8,950.2	3.5
168	368,472	378,051	410,115	385,546.0	21,809.8	5.7

Note: Cell counting using the Accuri C6 Cytometer was carried out with 100µL of each sample.

Supplementary Table 2. Raw cell counts data using the Neubauer chamber.

Time (h)	Replicate 1	Replicate 2	Replicate 3	Mean	Standard Deviation	Coefficient of variation (%)
0	2.25	1	1.25	1.5	0.7	44.1
24	6	5.5	4.25	5.3	0.9	17.2
48	9.25	8.5	7.75	8.5	0.8	8.8
72	28.25	30.75	33.75	30.9	2.8	8.9
96	43.5	46	54.5	48.0	5.8	12.0
108	82.25	85.5	73.5	80.4	6.2	7.7
120	115	136	64.5	105.2	36.8	34.9
132	135	100	157.5	130.8	29.0	22.1
144	210	252.5	287.5	250.0	38.8	15.5
168	510	395	560	488.3	84.6	17.3

Note: The numbers are the average of four Neubauer chamber quadrants.

Supplementary Table 3. Raw cell counts data using the Coulter Counter Analyser Cell Counter (Beckman Coulter).

Time (h)	Replicate 1	Replicate 2	Replicate 3	Mean	Standard Deviation	Coefficient of variation (%)
0	19,600	16,800	12,000	16,133.3	3,843.6	23.8
24	42,400	47,600	44,400	44,800.0	2,623.0	5.9
48	106,800	98,600	94,400	99,933.3	6,306.6	6.3
72	257,600	280,400	240,400	259,466.7	20,065.2	7.7
96	450,000	486,000	452,800	462,933.3	20,025.3	4.3
108	614,800	669,600	607,200	630,533.3	34,045.5	5.4
120	1,308,000	1,153,000	1,174,000	1,211,666.7	84,085.3	6.9
132	1,504,000	1,556,000	1,706,000	1,588,666.7	104,887.2	6.6
144	3,108,000	3,067,000	3,212,000	3,129,000.0	74,746.2	2.4
168	5,120,000	5,758,000	5,416,000	5,431,333.3	319,276.3	5.9

Note: Number of cells per mililiter.

Supplementary Table 4. Raw data from CFSE MFI measurements using the Accuri C6 Cytometer (BD Biosciences).

Time (h)	Replicate 1	Replicate 2	Replicate 3	Mean	Standard Deviation	Coefficient of variation (%)
0	1,272,412	1,212,068	1,222,749	1,235,742.9	32,202.0	2.6
24	428,813	411,320	427,511	422,548.0	9,745.2	2.3
48	122,389	141,198	140,890	134,825.9	10,771.5	8.0
72	44,798	46,260	46,366	45,807.9	876.6	1.9
96	28,317	29,340	27,947	28,534.5	721.6	2.5
108	17,837	17,831	18,338	18,002.0	290.6	1.6
120	10,163	11,582	11,057	10,934.3	717.6	6.6
132	7,844	7,674	6,841	7,453.0	536.6	7.2
144	3,852	3,902	4,175	3,976.3	173.6	4.4
168	2,955	2,846	2,885	2,895.2	55.6	1.9

Note: The MFI was measured from 4000 event from the single cells gate .

6. Final conclusions

In the first chapter of this thesis, our studies on ENC1 and human glioma progression show that ENC1 displays tumor suppression properties in U87MG human glioma cell line, ENC1 expression is upregulated during human glioma progression and ENC1 expression may be used as a biomarker for glioblastoma patients prognosis. The second chapter describes the identification and characterization of a peptide that is efficiently internalized into hGBM cells, and shows promise as a new tool for glioma therapeutic development. Finally, the third chapter describes described an alternative method for generating growth curves of adherent cells based on CFSE signal decay upon cell proliferation.

REFERENCIAS

Alberici, Luca, Lise Roth, Kazuki N Sugahara, Lilach Agemy, Venkata R Kotamraju, Tambet Teesalu, Claudio Bordignon, Catia Traversari, Gian-Paolo Rizzardi, and Erkki Ruoslahti. 2013. “De Novo Design of a Tumor-Penetrating Peptide.” *Cancer Research* 73 (2). NIH Public Access: 804–12. doi:10.1158/0008-5472.CAN-12-1668.

Alifieris, Constantinos, and Dimitrios T. Trafalis. 2015. “Glioblastoma Multiforme: Pathogenesis and Treatment.” *Pharmacology & Therapeutics* 152: 63–82. doi:10.1016/j.pharmthera.2015.05.005.

An, Sai, Xutao Jiang, Jiashu Shi, Xi He, Jianfeng Li, Yubo Guo, Yu Zhang, Haojun Ma, Yifei Lu, and Chen Jiang. 2015. “Single-Component Self-Assembled RNAi Nanoparticles Functionalized with Tumor-Targeting iNGR Delivering Abundant siRNA for Efficient Glioma Therapy.” *Biomaterials* 53: 330–40. doi:10.1016/j.biomaterials.2015.02.084.

Arap, Marco A., Johanna Lahdenranta, Paul J. Mintz, Amin Hajitou, Álvaro S. Sarkis, Wadih Arap, and Renata Pasqualini. 2004. “Cell Surface Expression of the Stress Response Chaperone GRP78 Enables Tumor Targeting by Circulating Ligands.” *Cancer Cell* 6 (3): 275–84. doi:10.1016/j.ccr.2004.08.018.

Begum, Julfa, William Day, Carl Henderson, Sukhveer Purewal, Joana Cerveira, Huw Summers, Paul Rees, Derek Davies, and Andrew Filby. 2013. “A Method for Evaluating the Use of Fluorescent Dyes to Track Proliferation in Cell Lines by Dye Dilution.” *Cytometry Part A* 83 (12): 1085–95. doi:10.1002/cyto.a.22403.

Bi, Yunke, Lisha Liu, Yifei Lu, Tao Sun, Chen Shen, Xinli Chen, Qinjun Chen, et al. 2016. “T7 Peptide-Functionalized PEG-PLGA Micelles Loading with Carmustine for Targeting Therapy of Glioma.” *ACS Applied Materials & Interfaces*, July. American Chemical Society , acsami.6b05572. doi:10.1021/acsami.6b05572.

Cardó-Vila, Marina, Amado J Zurita, Ricardo J Giordano, Jessica Sun, Roberto Rangel, Liliana Guzman-Rojas, Cristiane D Anobom, et al. 2008. “A Ligand Peptide Motif Selected from a Cancer Patient Is a Receptor-Interacting Site within Human Interleukin-11.” *PloS One* 3 (10). Public Library of Science: e3452. doi:10.1371/journal.pone.0003452.

Castilho, Leda, Angela Moraes, Elisabeth Augusto, and Mike Butler. 2008. *Animal Cell Technology - From Biopharmaceuticals to Gene Therapy*. 1st ed. Taylor & Francis. doi:10.4324/9780203895160.

Cates, Charles C, Angelo D Arias, Lynn S Nakayama Wong, Michael W Lamé, Maxim Sidorov, Geraldine Cayanan, Douglas J Rowland, et al. 2016.

"Regression/eradication of Gliomas in Mice by a Systemically-Deliverable ATF5 Dominant-Negative Peptide." *Oncotarget* 7 (11). Impact Journals, LLC: 12718–30. doi:10.18632/oncotarget.7212.

Chan, Andrew K, Harjus S Birk, Ethan A Winkler, Jennifer A Viner, Jennie W Taylor, and Michael W McDermott. 2016. "Stability of Programmable Shunt Valve Settings with Simultaneous Use of the Optune Transducer Array: A Case Report." *Curēus* 8 (7). Cureus Inc.: e675. doi:10.7759/cureus.675.

Chang, W L William, Veronica Kirchoff, Gregory S Pari, and Peter A Barry. 2002. "Replication of Rhesus Cytomegalovirus in Life-Expanded Rhesus Fibroblasts Expressing Human Telomerase." *Journal of Virological Methods* 104: 135–46. www.elsevier.com/locate/jviromet.

Chaubey, Nidhi, and Siddhartha Sankar Ghosh. 2014. "Overexpression of Granulocyte Macrophage Colony Stimulating Factor in Breast Cancer Cells Leads Towards Drug Sensitization." https://link.springer.com/content/pdf/10.1007%2Fs12010-014-1373-5.pdf.

Choi, Jina, Eun Sung Yang, Kiweon Cha, John Whang, Woo-Jung Choi, Shalom Avraham, and Tae-Aug Kim. 2014. "The Nuclear Matrix Protein, NRP/B, Acts as a Transcriptional Repressor of E2F-Mediated Transcriptional Activity." *Journal of Cancer Prevention* 19 (3): 187–98. doi:10.15430/JCP.2014.19.3.187.

Chung, Soobin, Seol-Hee Kim, Yuri Seo, Sook-Kyung Kim, and Ji Youn Lee. 2017. "Quantitative Analysis of Cell Proliferation by a Dye Dilution Assay: Application to Cell Lines and Cocultures." *Cytometry Part A* 91 (7). Wiley-Blackwell: 704–12. doi:10.1002/cyto.a.23105.

Degaki, Theri Leica, Marcos Angelo Almeida Demasi, and Mari Cleide Sogayar. 2009. "Overexpression of Nrp/b (Nuclear Restrict Protein in Brain) Suppresses the Malignant Phenotype in the C6/ST1 Glioma Cell Line." *The Journal of Steroid Biochemistry and Molecular Biology* 117 (4–5): 107–16. doi:10.1016/j.jsbmb.2009.07.009.

Dey, Joyoti, Adrian M Dubuc, Kyle D Pedro, Derek Thirstrup, Brig Mecham, Paul A Northcott, Xiaochong Wu, et al. 2013. "MyoD Is a Tumor Suppressor Gene in Medulloblastoma." *Cancer Research* 73 (22). NIH Public Access: 6828–37. doi:10.1158/0008-5472.CAN-13-0730-T.

Ellerby, H. Michael, Wadih Arap, Lisa M. Ellerby, Renate Kain, Rebecca Andrusiak, Gabriel Del Rio, Stanislaw Krajewski, et al. 1999. "Anti-Cancer Activity of Targeted pro-Apoptotic Peptides." *Nature Medicine* 5 (9). Nature Publishing Group: 1032–38. doi:10.1038/12469.

Fan, Shaohua, Yanyan Wang, Ning Sheng, Ying Xie, Jun Lu, Zifeng Zhang, Qun Shan,

et al. 2018. “Low Expression of ENC1 Predicts a Favorable Prognosis in Patients with Ovarian Cancer.” *Journal of Cellular Biochemistry*, August. doi:10.1002/jcb.27447.

Feng, Jie, Lichuan Hong, Yonggang Wu, Chuzhong Li, Hong Wan, Guilin Li, Yilin Sun, et al. 2014. “Identification of a Subtype-Specific ENC1 Gene Related to Invasiveness in Human Pituitary Null Cell Adenoma and Oncocytomas.” *Journal of Neuro-Oncology* 119 (2): 307–15. doi:10.1007/s11060-014-1479-1.

Freshney, R. Ian. 2010. *Culture of Animal Cells*. 6th ed. Hoboken, NJ, USA: John Wiley & Sons, Inc. doi:10.1002/9780470649367.

Fujita, Manabu, Yoichi Furukawa, Tatsuhiko Tsunoda, Toshihiro Tanaka, Michio Ogawa, and Yusuke Nakamura. 2001. “Up-Regulation of the Ectodermal-Neural Cortex 1 (ENC1) Gene, a Downstream Target of the {beta}-Catenin/T-Cell Factor Complex, in Colorectal Carcinomas.” *Cancer Res.* 61 (21): 7722–26. http://cancerres.aacrjournals.org/content/61/21/7722.long.

Gao, Changshou, Shenlan Mao, Henrik J Ditzel, Lauge Farnaes, Peter Wirsching, Richard A Lerner, and Kim D Janda. 2002. “A Cell-Penetrating Peptide from a Novel pVII-pIX Phage-Displayed Random Peptide Library.” *Bioorganic & Medicinal Chemistry* 10 (12): 4057–65. http://www.ncbi.nlm.nih.gov/pubmed/12413859.

Ghosh, Mila, Puja Sakhuja, Shivendra Singh, and Anil K Agarwal. 2013. “p53 and Beta-Catenin Expression in Gallbladder Tissues and Correlation with Tumor Progression in Gallbladder Cancer.” *Saudi Journal of Gastroenterology : Official Journal of the Saudi Gastroenterology Association* 19 (1). Wolters Kluwer -- Medknow Publications: 34–39. doi:10.4103/1319-3767.105922.

Giordano, Ricardo J., Marina Card?-Vila, Johanna Lahdenranta, Renata Pasqualini, and Wadih Arap. 2001. “Biopanning and Rapid Analysis of Selective Interactive Ligands.” *Nature Medicine* 7 (11). Nature Publishing Group: 1249–53. doi:10.1038/nm1101-1249.

Goldman, Elisheva B, Alla Zak, Reshef Tenne, Elena Kartvelishvily, Smadar Levin-Zaidman, Yoav Neumann, Raluca Stiubea-Cohen, Aaron Palmon, Avi-Hai Hovav, and Doron J Aframian. 2015. “Biocompatibility of Tungsten Disulfide Inorganic Nanotubes and Fullerene-like Nanoparticles with Salivary Gland Cells.” *Tissue Engineering. Part A* 21 (5–6). Mary Ann Liebert, Inc.: 1013–23. doi:10.1089/ten.TEA.2014.0163.

Greenblatt, M S, W P Bennett, M Hollstein, and C C Harris. 1994. “Mutations in the p53 Tumor Suppressor Gene: Clues to Cancer Etiology and Molecular Pathogenesis.” *Cancer Research* 54 (18). American Association for Cancer Research: 4855–78. http://www.ncbi.nlm.nih.gov/pubmed/8069852.

Gupta, Vandana A, and Alan H Beggs. 2014. “Kelch Proteins: Emerging Roles in Skeletal Muscle Development and Diseases.” *Skeletal Muscle* 4 (January): 11. doi:10.1186/2044-5040-4-11.

Hajitou, Amin, Martin Trepel, Caroline E. Lilley, Suren Soghomonyan, Mian M. Alauddin, Frank C. Marini, Bradley H. Restel, et al. 2006. “A Hybrid Vector for Ligand-Directed Tumor Targeting and Molecular Imaging.” *Cell* 125 (2): 385–98. doi:10.1016/j.cell.2006.02.042.

Hammarsund, Marianne, Mikael Lerner, Chaoyong Zhu, Mats Merup, Monika Jansson, Gösta Gahrton, Hanneke Kluin-Nelemans, et al. 2004. “Disruption of a Novel Ectodermal Neural Cortex 1 Antisense Gene, ENC-1AS and Identification of ENC-1 Overexpression in Hairy Cell Leukemia.” *Human Molecular Genetics* 13 (23): 2925–36. doi:10.1093/hmg/ddh315.

Hernandez, M C, P J Andres-Barquin, I Holt, and M A Israel. 1998. “Cloning of Human ENC-1 and Evaluation of Its Expression and Regulation in Nervous System Tumors.” *Experimental Cell Research* 242 (2): 470–77. doi:10.1006/excr.1998.4109.

Hernandez, M C, P J Andres-Barquin, S Martinez, A Bulfone, J L Rubenstein, and M A Israel. 1997. “ENC-1: A Novel Mammalian Kelch-Related Gene Specifically Expressed in the Nervous System Encodes an Actin-Binding Protein.” *The Journal of Neuroscience : The Official Journal of the Society for Neuroscience* 17 (9): 3038–51. http://www.ncbi.nlm.nih.gov/pubmed/9096139.

Huynh, H. 2004. “Overexpression of Tumour Suppressor Retinoblastoma 2 Protein (pRb2/p130) in Hepatocellular Carcinoma.” *Carcinogenesis* 25 (8). Oxford University Press: 1485–94. doi:10.1093/carcin/bgh154.

Jiang, Li-hua, Nian-yun Yang, Xiao-lin Yuan, Yi-jie Zou, Feng-ming Zhao, Jian-ping Chen, Ming-yan Wang, and Da-xiang Lu. 2014. “Daucosterol Promotes the Proliferation of Neural Stem Cells.” *The Journal of Steroid Biochemistry and Molecular Biology* 140 (March). Pergamon: 90–99. doi:10.1016/J.JSBMB.2013.12.002.

Kantardjieff, Anne, and Weichang Zhou. 2013. “Mammalian Cell Cultures for Biologics Manufacturing.” In *Advances in Biochemical Engineering/biotechnology*, 139:1–9. doi:10.1007/10_2013_255.

Kay, Brian K., Alexei V. Kurakin, and Robin Hyde-DeRuyscher. 1998. “From Peptides to Drugs via Phage Display.” *Drug Discovery Today* 3 (8): 370–78. doi:10.1016/S1359-6446(98)01220-3.

Kim, T A, J Lim, S Ota, S Raja, R Rogers, B Rivnay, H Avraham, and S Avraham. 1998. “NRP/B, a Novel Nuclear Matrix Protein, Associates with p110(RB) and Is Involved

in Neuronal Differentiation." *The Journal of Cell Biology* 141 (3): 553–66. http://www.pubmedcentral.nih.gov/articlerender.fcgi?artid=2132755&tool=pmcentrez&rendertype=abstract.

Kim, Tae-Aug, Setsuo Ota, Shuxian Jiang, Linda M. Pasztor, Robert A. White, and Shalom Avraham. 2000. "Genomic Organization, Chromosomal Localization and Regulation of Expression of the Neuronal Nuclear Matrix Protein NRP/B in Human Brain Tumors." *Gene* 255 (1): 105–16. doi:10.1016/S0378-1119(00)00297-3.

Lee, N K. 2018. "Tumor Suppressor Genes." *Head & Neck* 14 (5): 407–14. Accessed September 21. http://www.ncbi.nlm.nih.gov/pubmed/1399577.

Lesniak, Maciej S, and Henry Brem. 2004. "Targeted Therapy for Brain Tumours." *Nature Reviews. Drug Discovery* 3 (6): 499–508. doi:10.1038/nrd1414.

Liang, Xing-Qun, Hava Karsenty Avraham, Shuxian Jiang, and Shalom Avraham. 2004. "Genetic Alterations of the NRP/B Gene Are Associated with Human Brain Tumors." *Oncogene* 23 (35): 5890–5900. doi:10.1038/sj.onc.1207776.

Liu, Yayuan, Ling Mei, Chaoqun Xu, Qianwen Yu, Kairong Shi, Li Zhang, Yang Wang, et al. 2016. "Dual Receptor Recognizing Cell Penetrating Peptide for Selective Targeting, Efficient Intratumoral Diffusion and Synthesized Anti-Glioma Therapy." *Theranostics* 6 (2): 177–91. doi:10.7150/thno.13532.

Liu, Yayuan, Ling Mei, Qianwen Yu, Chaoqun Xu, Yue Qiu, Yuting Yang, Kairong Shi, et al. 2015. "Multifunctional Tandem Peptide Modified Paclitaxel-Loaded Liposomes for the Treatment of Vasculogenic Mimicry and Cancer Stem Cells in Malignant Glioma." *ACS Applied Materials & Interfaces* 7 (30): 16792–801. doi:10.1021/acsami.5b04596.

Louis, David N., Arie Perry, Guido Reifenberger, Andreas von Deimling, Dominique Figarella-Branger, Webster K. Cavenee, Hiroko Ohgaki, Otmar D. Wiestler, Paul Kleihues, and David W. Ellison. 2016. "The 2016 World Health Organization Classification of Tumors of the Central Nervous System: A Summary." *Acta Neuropathologica* 131 (6). Springer Berlin Heidelberg: 803–20. doi:10.1007/s00401-016-1545-1.

Louis, David N, Hiroko Ohgaki, Otmar D Wiestler, Webster K Cavenee, Peter C Burger, Anne Jouvet, Bernd W Scheithauer, and Paul Kleihues. 2007. "The 2007 WHO Classification of Tumours of the Central Nervous System." *Acta Neuropathologica* 114 (2): 97–109. doi:10.1007/s00401-007-0243-4.

Lyons, A.Bruce, and Christopher R. Parish. 1994. "Determination of Lymphocyte Division by Flow Cytometry." *Journal of Immunological Methods* 171 (1): 131–37. doi:10.1016/0022-1759(94)90236-4.

Ma, Liang, Chi Nam Ignatius Pang, Simone S. Li, and Marc R. Wilkins. 2010. “Proteins Deleterious on Overexpression Are Associated with High Intrinsic Disorder, Specific Interaction Domains, and Low Abundance.” *Journal of Proteome Research* 9 (3). American Chemical Society: 1218–25. doi:10.1021/pr900693e.

Marx, Uwe. 2012. “Trends in Cell Culture Technology.” In *Advances in Experimental Medicine and Biology*, 745:26–46. doi:10.1007/978-1-4614-3055-1_3.

Mei, Ling, Qianyu Zhang, Yuting Yang, Qin He, and Huile Gao. 2014. “Angiopep-2 and Activatable Cell Penetrating Peptide Dual Modified Nanoparticles for Enhanced Tumor Targeting and Penetrating.” *International Journal of Pharmaceutics* 474 (1): 95–102. doi:10.1016/j.ijpharm.2014.08.020.

Moriya, Hisao. 2015. “Quantitative Nature of Overexpression Experiments.” *Molecular Biology of the Cell* 26 (22). American Society for Cell Biology: 3932–39. doi:10.1091/mbc.E15-07-0512.

Ohgaki, Hiroko, and Paul Kleihues. 2005. “Epidemiology and Etiology of Gliomas.” *Acta Neuropathologica* 109 (1): 93–108. doi:10.1007/s00401-005-0991-y.

Oka, Tetsuo, Kazuhiko Kurozumi, Yosuke Shimazu, Tomotsugu Ichikawa, Joji Ishida, Yoshihiro Otani, Toshihiko Shimizu, et al. 2016. “A Super Gene Expression System Enhances the Anti-Glioma Effects of Adenovirus-Mediated REIC/Dkk-3 Gene Therapy.” *Scientific Reports* 6: 33319. doi:10.1038/srep33319.

Omuro, Antonio, and Lisa M DeAngelis. 2013. “Glioblastoma and Other Malignant Gliomas.” *JAMA* 310 (17): 1842. doi:10.1001/jama.2013.280319.

Ostrom, Quinn T, Luc Bauchet, Faith G Davis, Isabelle Deltour, James L Fisher, Chelsea Eastman Langer, Melike Pekmezci, et al. 2014. “The Epidemiology of Glioma in Adults: A ‘state of the Science’ review.” *Neuro-Oncology* 16 (7). Oxford University Press: 896–913. doi:10.1093/neuonc/nou087.

Ostrom, Quinn T, Haley Gittleman, Jordonna Fulop, Max Liu, Rachel Blanda, Courtney Kromer, Yingli Wolinsky, Carol Kruchko, and Jill S Barnholtz-Sloan. 2015. “CBTRUS Statistical Report: Primary Brain and Central Nervous System Tumors Diagnosed in the United States in 2008-2012.” *Neuro-Oncology* 17 Suppl 4 (Suppl 4). Oxford University Press: iv1-iv62. doi:10.1093/neuonc/nov189.

Parker, Seth J, and Christian M Metallo. 2015. “Metabolic Consequences of Oncogenic IDH Mutations.” *Pharmacology & Therapeutics*, May. doi:10.1016/j.pharmthera.2015.05.003.

Pasqualini, Renata, Randall E Millikan, Dawn R Christianson, Marina Cardó-Vila, Wouter H P Driessen, Ricardo J Giordano, Amin Hajitou, et al. 2015. “Targeting the Interleukin-11 Receptor α in Metastatic Prostate Cancer: A First-in-Man Study.”

Cancer 121 (14). Wiley-Blackwell: 2411–21. doi:10.1002/cncr.29344.

Pfaffl, M W. 2001. “A New Mathematical Model for Relative Quantification in Real-Time RT-PCR.” *Nucleic Acids Research* 29 (9): e45. http://www.pubmedcentral.nih.gov/articlerender.fcgi?artid=55695&tool=pmcentrez&rendertype=abstract.

Philips, Thomas, and Jeffrey D. Rothstein. 2017. “Oligodendroglia: Metabolic Supporters of Neurons.” *Journal of Clinical Investigation* 127 (9): 3271–80. doi:10.1172/JCI90610.

Platten, Michael, Lukas Bunse, Wolfgang Wick, and Theresa Bunse. 2016. “Concepts in Glioma Immunotherapy.” *Cancer Immunology, Immunotherapy : CII*, July. doi:10.1007/s00262-016-1874-x.

Polyak, K, Y Xia, J L Zweier, K W Kinzler, and B Vogelstein. 1997. “A Model for p53-Induced Apoptosis.” *Nature* 389 (6648): 300–305. doi:10.1038/38525.

Quah, Ben J C, Hilary S Warren, and Christopher R Parish. 2007. “Monitoring Lymphocyte Proliferation in Vitro and in Vivo with the Intracellular Fluorescent Dye Carboxyfluorescein Diacetate Succinimidyl Ester.” doi:10.1038/nprot.2007.296.

Quah, Benjamin J C, and Christopher R Parish. 2012. “New and Improved Methods for Measuring Lymphocyte Proliferation in Vitro and in Vivo Using CFSE-like Fluorescent Dyes.” doi:10.1016/j.jim.2012.02.012.

Rabah, Dania, Steve Grant, Check Ma, and Daniel H Conrad. 2001. “Synthesis Bryostatin-1 Specifically Inhibits In Vitro IgE Bryostatin-1 Specifically Inhibits In Vitro IgE Synthesis 1.” *J Immunol References The Journal of Immunology* 167: 4910–18. doi:10.4049/jimmunol.167.9.4910.

Romar, George A., Thomas S. Kupper, and Sherrie J. Divito. 2016. “Research Techniques Made Simple: Techniques to Assess Cell Proliferation.” *Journal of Investigative Dermatology* 136 (1). Elsevier: e1–7. doi:10.1016/J.JID.2015.11.020.

Rosen, Eliot M, and Michael J Pishvaian. 2014. “Targeting the BRCA1/2 Tumor Suppressors.” *Current Drug Targets* 15 (1): 17–31. http://www.ncbi.nlm.nih.gov/pubmed/24387337.

Seng, Seyha, Hava Karsenty Avraham, Shuxian Jiang, Suping Yang, Masayuki Sekine, Noam Kimelman, Huchun Li, and Shalom Avraham. 2007. “The Nuclear Matrix Protein, NRP/B, Enhances Nrf2-Mediated Oxidative Stress Responses in Breast Cancer Cells.” *Cancer Research* 67 (18): 8596–8604. doi:10.1158/0008-5472.CAN-06-3785.

Shi, Kairong, Yang Long, Chaoqun Xu, Yang Wang, Yue Qiu, Qianwen Yu, Yayuan Liu,

et al. 2015. “Liposomes Combined an Integrin αvβ3-Specific Vector with pH-Responsible Cell-Penetrating Property for Highly Effective Antiglioma Therapy through the Blood-Brain Barrier.” *ACS Applied Materials & Interfaces*, September. American Chemical Society. doi:10.1021/acsami.5b06429.

Smith, G P. 1985. “Filamentous Fusion Phage: Novel Expression Vectors That Display Cloned Antigens on the Virion Surface.” *Science (New York, N.Y.)* 228 (4705): 1315–17. http://www.ncbi.nlm.nih.gov/pubmed/4001944.

Smith, Tracey L, Ziqiang Yuan, Marina Cardó-Vila, Carmen Sanchez Claros, Asha Adem, Min-Hui Cui, Craig A Branch, et al. 2016. “AAVP Displaying Octreotide for Ligand-Directed Therapeutic Transgene Delivery in Neuroendocrine Tumors of the Pancreas.” *Proceedings of the National Academy of Sciences of the United States of America* 113 (9). National Academy of Sciences: 2466–71. doi:10.1073/pnas.1525709113.

Sonabend, Adam M, Ilya V Ulasov, and Maciej S Lesniak. 2007. “Gene Therapy Trials for the Treatment of High-Grade Gliomas.” *Gene Therapy & Molecular Biology* 11 (A): 79–92. http://www.pubmedcentral.nih.gov/articlerender.fcgi?artid=1913943&tool=pmcentrez&rendertype=abstract.

Stacey, Glyn. 2012. “Current Developments in Cell Culture Technology.” In *Advances in Experimental Medicine and Biology*, edited by N. Cohen, I.R., Lajtha, A., Lambris, J.D., Paoletti, R., Rezaei, 745:1–13. doi:10.1007/978-1-4614-3055-1_1.

Staquicini, Fernanda I, Michael G Ozawa, Catherine A Moya, Wouter H P Driessen, E Magda Barbu, Hiroyuki Nishimori, Suren Soghomonyan, et al. 2011. “Systemic Combinatorial Peptide Selection Yields a Non-Canonical Iron-Mimicry Mechanism for Targeting Tumors in a Mouse Model of Human Glioblastoma.” *The Journal of Clinical Investigation* 121 (1). American Society for Clinical Investigation: 161–73. doi:10.1172/JCI44798.

Sugahara, Kazuki N, Tambet Teesalu, Priya Prakash Karmali, Venkata Ramana Kotamraju, Lilach Agemy, Olivier M Girard, Douglas Hanahan, Robert F Mattrey, and Erkki Ruoslahti. 2009. “Tissue-Penetrating Delivery of Compounds and Nanoparticles into Tumors.” *Cancer Cell* 16 (6). NIH Public Access: 510–20. doi:10.1016/j.ccr.2009.10.013.

Vasile, Flora, Elena Dossi, and Nathalie Rouach. 2017. “Human Astrocytes: Structure and Functions in the Healthy Brain.” *Brain Structure and Function* 222 (5): 2017–29. doi:10.1007/s00429-017-1383-5.

Verhaak, Roel G W, Katherine A Hoadley, Elizabeth Purdom, Victoria Wang, Yuan Qi, Matthew D Wilkerson, C Ryan Miller, et al. 2010. “Integrated Genomic Analysis Identifies Clinically Relevant Subtypes of Glioblastoma Characterized by

Abnormalities in PDGFRA, IDH1, EGFR, and NF1." *Cancer Cell* 17 (1). NIH Public Access: 98–110. doi:10.1016/j.ccr.2009.12.020.

Wang, Lei, Yongwei Hao, Haixia Li, Yalin Zhao, Dehui Meng, Dong Li, Jinjin Shi, Hongling Zhang, Zhenzhong Zhang, and Yun Zhang. 2015. "Co-Delivery of Doxorubicin and siRNA for Glioma Therapy by a Brain Targeting System: Angiopep-2-Modified Poly(lactic-Co-Glycolic Acid) Nanoparticles." *Journal of Drug Targeting* 23 (9). Informa Healthcare: 832–46. doi:10.3109/1061186X.2015.1025077.

Wei, Xiaoli, Jie Gao, Changyou Zhan, Cao Xie, Zhilan Chai, Danni Ran, Man Ying, Ping Zheng, and Weiyue Lu. 2015. "Liposome-Based Glioma Targeted Drug Delivery Enabled by Stable Peptide Ligands." *Journal of Controlled Release : Official Journal of the Controlled Release Society* 218 (September): 13–21. doi:10.1016/j.jconrel.2015.09.059.

Wolf, Susanne A., H.W.G.M. Boddeke, and Helmut Kettenmann. 2017. "Microglia in Physiology and Disease." *Annual Review of Physiology* 79 (1): 619–43. doi:10.1146/annurev-physiol-022516-034406.

Wu, Chien-Hsun, I-Ju Liu, Ruei-Min Lu, and Han-Chung Wu. 2016. "Advancement and Applications of Peptide Phage Display Technology in Biomedical Science." *Journal of Biomedical Science* 23 (1): 8. doi:10.1186/s12929-016-0223-x.

Yao, Hui, Kaiyuan Wang, Yi Wang, Shanshan Wang, Jianfeng Li, Jinning Lou, Liya Ye, Xueying Yan, Weiyue Lu, and Rongqin Huang. 2015. "Enhanced Blood–brain Barrier Penetration and Glioma Therapy Mediated by a New Peptide Modified Gene Delivery System." *Biomaterials* 37: 345–52. doi:10.1016/j.biomaterials.2014.10.034.

Yokota, Naoki, Todd G Mainprize, Michael D Taylor, Tomohiko Kohata, Michael Loreto, Shigeo Ueda, Wieslaw Dura, Wiesia Grajkowska, John S Kuo, and James T Rutka. 2004. "Identification of Differentially Expressed and Developmentally Regulated Genes in Medulloblastoma Using Suppression Subtraction Hybridization." *Oncogene* 23 (19): 3444–53. doi:10.1038/sj.onc.1207475.

Zahid, Maliha, and Paul D Robbins. 2012. "Protein Transduction Domains: Applications for Molecular Medicine." *Current Gene Therapy* 12 (5): 374–80. http://www.ncbi.nlm.nih.gov/pubmed/22920684.

Zahid, Maliha, and Paul D Robbins. 2015. "Cell-Type Specific Penetrating Peptides: Therapeutic Promises and Challenges." *Molecules (Basel, Switzerland)* 20 (7). Multidisciplinary Digital Publishing Institute: 13055–70. doi:10.3390/molecules200713055.

Zeisel, Amit, Ana B Muñoz-Manchado, Simone Codeluppi, Peter Lönnerberg, Gioele La Manno, Anna Juréus, Sueli Marques, et al. 2015. "Brain Structure. Cell Types in the

Mouse Cortex and Hippocampus Revealed by Single-Cell RNA-Seq." *Science (New York, N.Y.)* 347 (6226). American Association for the Advancement of Science: 1138–42. doi:10.1126/science.aaa1934.

Zhang, Bo, Yujie Zhang, Ziwei Liao, Ting Jiang, Jingjing Zhao, Yanyan Tuo, Xiaojian She, et al. 2015. "UPA-Sensitive ACPP-Conjugated Nanoparticles for Multi-Targeting Therapy of Brain Glioma." *Biomaterials* 36: 98–109. doi:10.1016/j.biomaterials.2014.09.008.

Zhang, Li, Yanyu Zhang, Lingyu Tai, Kuan Jiang, Cao Xie, Zhuoquan Li, Yao-Zhong Lin, Gang Wei, Weiyue Lu, and Weisan Pan. 2016. "Functionalized Cell Nucleus-Penetrating Peptide Combined with Doxorubicin for Synergistic Treatment of Glioma." *Acta Biomaterialia* 42: 90–101. doi:10.1016/j.actbio.2016.06.031.

Zhang, Ye, Steven A. Sloan, Laura E. Clarke, Christine Caneda, Colton A. Plaza, Paul D. Blumenthal, Hannes Vogel, et al. 2015. "Purification and Characterization of Progenitor and Mature Human Astrocytes Reveals Transcriptional and Functional Differences with Mouse." *Neuron* 89 (1): 37–53. doi:10.1016/j.neuron.2015.11.013.

Zheng, Chuanyi, Chunyang Ma, Enqi Bai, Kun Yang, and Ruxiang Xu. 2015. "Transferrin and Cell-Penetrating Peptide Dual-Functioned Liposome for Targeted Drug Delivery to Glioma." *International Journal of Clinical and Experimental Medicine* 8 (2). e-Century Publishing Corporation: 1658–68. http://www.ncbi.nlm.nih.gov/pubmed/25932094.

Zou, Yan, Fenghua Meng, Chao Deng, and Zhiyuan Zhong. 2016. "Robust, Tumor-Homing and Redox-Sensitive Polymersomal Doxorubicin: A Superior Alternative to Doxil and Caelyx?" *Journal of Controlled Release : Official Journal of the Controlled Release Society*, August. doi:10.1016/j.jconrel.2016.08.022.

SÚMULA CURRICULAR

1. DADOS PESSOAIS

Nome: Túlio Felipe Pereira
Local e data de nascimento: Pouso Alegre/MG, 21 de maio de 1986

2. EDUCAÇÃO

Universidade Federal de Alfenas – Alfenas/MG
De 08/2004 a 04/2010
Graduação em Farmácia

3. FORMAÇÃO COMPLEMENTAR

Invitare Pesquisa Clínica – São Paulo/SP
60 horas
Capacitação em Pesquisa Clínica – 2012

ICTQ – São Paulo/SP
400 horas
Pós-graduação lato sensu
Assuntos Regulatório na Indústria Farmacêutica - 2012

4. OCUPAÇÃO

Grupo Cimed - Pouso Alegre/MG
De 04/2010 a 01/2011
Analista de Garantia de Qualidade

Instituto Cláudia Marques de Pesquisa e Desenvolvimento - Pouso Alegre/MG
De 01/2011 a 11/2012
Monitor de Etapa Clínica de Estudos de Bioequivalência

Bolsista de Doutorado, CNPq e FAPESP
De 08/2013 a 09/2018
Departamento de Bioquímica – Instituto de Química - Universidade de São Paulo.

5. PUBLICAÇÕES (Artigos Completos e Resumos em Congressos)

Galatro TF, Holtman IR, Lerario AM, Vainchtein ID, Brouwer N, Sola PR, Veras MM, **Pereira TF**, Leite REP, Möller T, Wes PD, Sogayar MC, Laman JD, den Dunnen W, Pasqualucci CA, Oba-Shinjo SM, Boddeke EWGM, Marie SKN, Eggen BJL. Transcriptomic Analysis of Purified Human Cortical Microglia Reveals Age-Associated Changes. Nat. Neurosci. 2017; 20: 1162–1171; DOI:10.1038/nn.4597.

(Submetido em 2 de Agosto de 2018)
Pereira, TF; Levin, G; DeOcesano-Pereira, C; Coadaglio, AS; Fujita, A; Tonso, A; Sogayar, MC. Counting-free fluorescence-based method to generate growth curves of adherent cell cultures. **Cytometry Part A.**

(Em preparação)
Pereira TF, Camargo L, Machado RAC, Marie SKN, Demasi MA, Sogayar MC. Upregulation of tumor suppressor Ectodermal-neural cortex 1 protein (ENC1) during human glioma progression is associated with unfavorable patient prognosis.

(Em preparação)
Pereira TF, Caodaglio AS, Staquicini F, Arap W, Pasqualini R, Sogayar MC. Human glioblastoma cells internalize the LHTNELQ peptide for targeted drug delivery.

Resumos em congressos

Pereira TF, Astorino Filho R, Caodaglio AS, Marie SKN, Sogayar MC. Identification of cell penetrating peptides in human glioblastoma cells using Phage Display. PEGS Boston - Protein Engineering Summit. Boston, USA. 2015.

Galatro TFA, Holtman IR, Brouwer N, Sola P, Reis GN, Vainchtein ID, Veras M, **Pereira TF**, Pasqualucci C, Sogayar MC, Boddeke EW, Marie SKN, Eggen BJ. Human Microglia Transcriptome and Cross-species Analysis.Bilbao, Spain 2015

Ribeiro IS, **Pereira TF**, Costa CM, Alencar SM, Ikegaki M. Analysis of chemical composition and biological properties of red propolis produced by *Apis mellifera* from Alagoas state, Brazil. Federation of Experimental Biology Societies meeting. São Paulo, Brazil 2005.

Pereira TF, Ribeiro IS, Costa CM, Alencar SM, Ikegaki M. Analysis of chemical profile and antibiotic activity of White Propolis. Scientific Iniciantion Workshop. Alfenas, Brazil 2005.